Results and Discussion

Chapter-4

4. RESULTS AND DISCUSSION

4.1. Biocomputational identification of small RNAs

The computational identification of small noncoding RNA genes represents one of the challenging problems in computational biology. A set of 8 sRNA candidates SprA, SprB, SprC, SprD, SprE (which was later reported to be a rRNA fragment and not a sRNA (Svetlana Chabelskaya and Brice Felden unpublished results)), SprX (sRNA expressed from the opposite strand of SprE), SprF, SprG identified *in silico* and expressed within the intergenic regions of the pathogenicity islands of Methicillin Resistant *Staphylococcus aureus* (MRSA) N315 strain (Pichon & Felden, 2005; Bohn

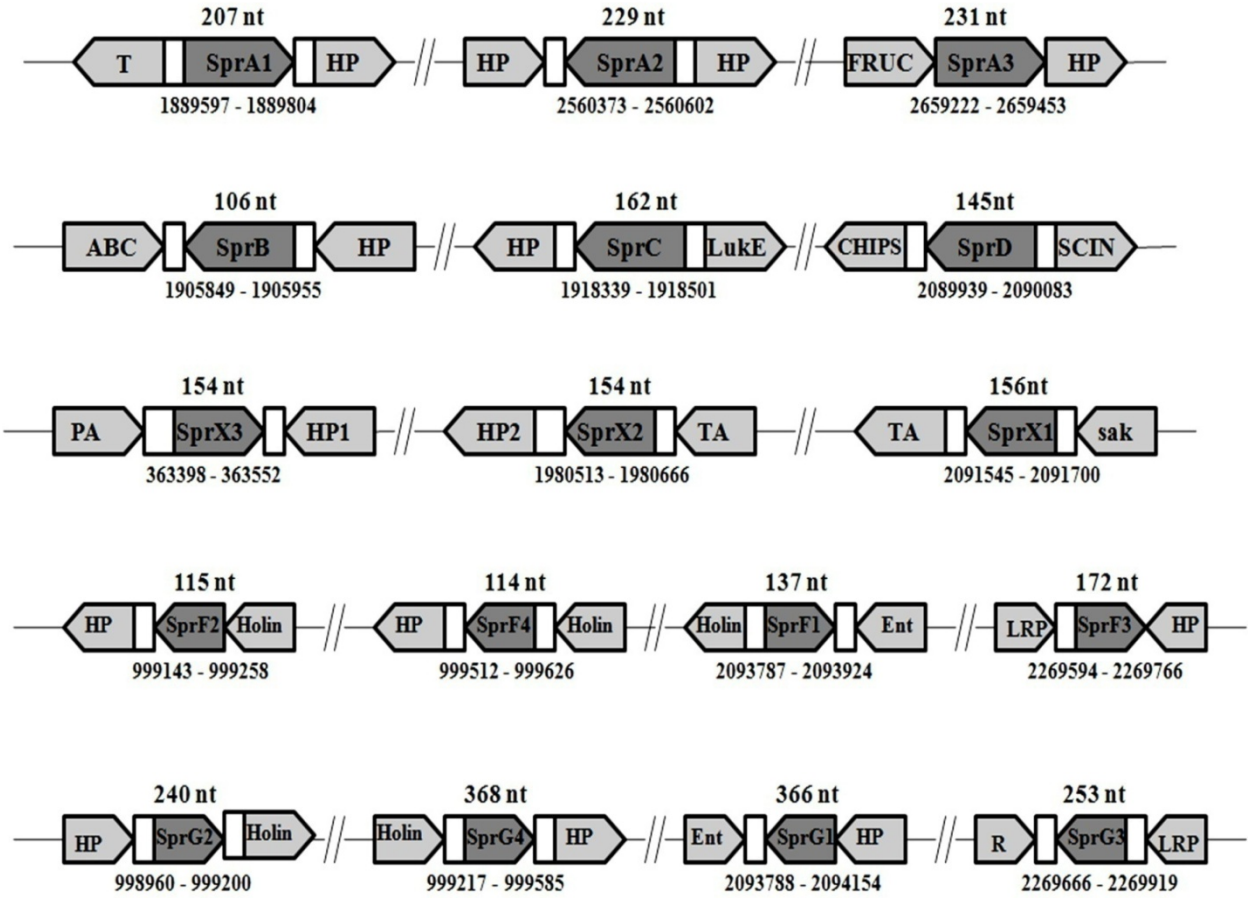

Fig. 13. Genomic location of SprA-G in *S. aureus* Newman. Schematic representations of the genetic organization of SprA, SprB, SprC, SprD, SprX, SprF, SprG loci from *S. aureus* strain Newman. The flanking ORFs, orientation of Spr genes and nucleotide (nts) numbers correspond to those of strain Newman. T - Transposase; HP - Hypothetical protein; ABC - lantibiotic ABC transporter ATP-binding protein; FRUC - Fructose-1,6 bisphosphatase; LukE - Leukocidin E precursor; SCIN - Staphylococcal complement inhibitor; CHIPS - Chemotaxis inhibiting protein; ent - Enterotoxin type A precursor; LRP - Lytic regulatory protein; R - Resolvase; PA – Phage amidase; sak - Staphylokinase precursor.

et al., 2010) were used to find the homologues sequence in the clinical isolate Methicillin Susceptible *Staphylococcus aureus* (MSSA) strain Newman (Fig. 13). All these ncRNAs were further taken for *in silico* analysis.

4.1.1. Identification of small RNAs within the IGRs of *S. aureus* Newman

Small RNA (sRNA) genes are flanked by protein coding genes. sRNAs present in the intergenic region(IGR) of *S. aureus* Newman were predicted by finding the putative promoter sequences and the rho independent transcription terminator by using online prediction tools Softberry BPROM and Erpin with default parameters respectively.

Later in 2015, Sassi *et al.,* established the Staphylococcal Regulatory RNA Database (SRD) which includes all the ncRNAs reported in *Staphylococcus* so far. This database contains information which includes small RNA's genetic locations and its co-ordinates, sequences, length, structure and provides link for the target prediction in several strains of human pathogen *Staphylococcus aureus* with *S. aureus* N315 as a reference strain. The predictions regarding the genetic locations, co-ordinates etc. that were made in this study were confirmed from this new database. Pathogenicity island encoded sRNAs in *S. aureus* strain Newman are summarized in Table 14.

4.1.2. *in silico* prediction of mRNA targets

Computational identification of sRNA targets is a complicated task, due to the base pairing of multiple discontinuous regions of the sRNA or mRNA leading to the high degree of uncertainty about the interaction. The sRNA controls the fate of mRNAs by base pairing with the target mRNAs (Wang *et al.,* 2015). There are several proposed features of sRNA: mRNA interactions that were taken into account for bioinformatic prediction of targets. Some of the selected features are the region of base pairing interaction of mRNAs and sRNA and a continuous base pairing with a minimum of 9 bp at one end of the paired region that were taken into consideration (Gottesman and Storz, 2010; Storz *et al.,* 2011). An extensive *in silico* analysis was performed using the various online target prediction tools such as TargetRNA1, TargetRNA2, RNA Predator, RNAup and IntaRNA for predicting mRNA targets for the sRNAs. The predicted targets for the analysed small RNAs are listed in Table 15.

Table 14. Pathogenicity island (PaIs) encoded small RNAs in *S. aureus* Newman.

sRNAs and its copy number		Co-ordinates	Strand	Length	Other names	Flanking genes
SprA (3)	SprA1	1889597-1889804	+	207	Teg8/ IGR1520/ sRNA285	Transposase and hypothetical protein
	SprA2	2560373-2560602	-	229	IGR2049/ IGR8bis/ Teg26as/ sRNA371	Hypothetical protein and hypothetical protein
	SprA3	2659222-2659453	+	231	IGR2125	Fructose-1,6 bisphosphatase and conserved hypothetical protein
SprB (1)	SprB	1905849-1905955	-	106	Teg9/ IGR18	Lantibiotic ABC transporter protein and hypothetical protein
SprC (1)	SprC	1918339-1918501	-	162	Teg10/ IGR18	Hypothetical protein and leukocidin LukE precursor
SprD (1)	SprD	2089939-2090083	-	145	Teg14/ sRNA300	Chemotaxis inhibiting protein CHIPS and Staphylococcal complement inhibitor SCIN
SprF (4)	SprF1	2093787-2093924	+	137	IGR1644/ Teg154/ sRNA309	Phage holin and enterotoxin type A precursor
	SprF2	999143-999258	-	115	Teg19a/ Teg102/ Sau02/ sRZN/ sRNA190	Hypothetical protein and putative holin like toxin
	SprF3	2269594-2269766	+	172	Teg19a/ RsaOS/ sRNA332	Lytic regulatory protein and hypothetical protein
	SprF4	999512-999626	-	114	Teg19a/ Teg102/ Sau02/ sRZN/ sRNA191	Hypothetical protein and putative holin like toxin
SprG	SprG1	2093788-2094154	-	366	sRNA310	Enterotoxin A and hypothetical protein
	SprG2	998960-999200	+	240	Teg19b	Hypothetical protein and putative holin like toxin
	SprG3	2269666-	-	253	Teg102/	Resolvase and lytic

(4)		2269919			Teg19b/ sRNA333	regulatory protein
	SprG4	999217-999585	+	368	Teg19b	Putative holin like toxin and hypothetical protein
SprX (3)	SprX1	2091551-2091700	-	156	RsaOR/ Ssr6/ Teg15/ sRNA299/ IGR12	Truncated phage amidase and staphylokinase precursor
	SprX2	1980518-1980666	-	154	RsaOR/ Ssr6/ Teg15/ sRNA292/ IGR12	Hypothetical protein and phage amidase
	SprX3	363398-363546	+	154	RsaOR/ Ssr6/ Teg15/ sRNA299	Phage amidase and hypothetical protein

Table 15. List of mRNA targets of Pathogenicity island encoded small RNAs in *S. aureus* Newman.

sRNA	Target mRNAs	P value	Energy
SprA1	oligopeptide transport system permease	0.001	-14.50
	N-acetyl muramoyl-L-alanine amidase precursor	0.007	-12.18
	methicillin resistance protein FemA	0.009	-11.69
	putative DNA-binding protein	0.011	-11.45
	membrane protein oxaA precursor	0.015	-10.78
	fatty acid biosynthesis transcriptional regulator	0.016	-10.71
	leukocidin LukE precursor	0.032	-9.37
	chaperonin GroEL	0.032	-9.32
	alpha-hemolysin precursor	0.034	-9.19
	ABC transporter ATP-binding protein	0.040	-8.84
SprB	hypothetical protein	0.000	-17.01
	oligopeptide ABC transporter ATP-binding protein	0.005	-12.71
	dihydrolipoamide dehydrogenase	0.005	-12.52
	oligopeptide transporter permease	0.007	-12.13
	uracil-DNA glycosylase	0.008	-11.82
	tandem lipoprotein	0.022	-10.12
	ribonuclease BN	0.025	-9.89
	ABC transporter ATP-binding protein VraF	0.040	-8.85
	acyl-CoA dehydrogenase-related protein	0.040	-8.84
	recombination factor protein RarA	0.041	-8.77
	clumping factor B	0.0075	Score: -64
	clumping factor A	Z score-3.14	-10.62
	staphylocoagulase	Z score-1.56	-8.16
	MmpL efflux pump	Z score-2.34	-9.90
	Quinolone resistance norA protein	Z score-1.61	-8.53
	hypothetical protein	0.002	-13.55

SprC	iron compound ABC transporter iron compound-binding protein	0.003	-13.4
	alkaline phosphatase III precursor	0.022	-10.08
	dimethyladenosine transferase	0.025	-9.89
	alanine racemase 2	0.035	-9.11
	threonine synthase	0.036	-9.08
	lactose phosphotransferase system repressor	0.043	-8.66
	uracil-DNA glycosylase	0.044	-8.62
SprD	fatty acid biosynthesis transcriptional regulator	0.000	-15.9
	exonuclease ABC subunit C	0.001	-15.08
	choline transporter	0.003	-13.31
	serine hydroxymethyltransferase	0.003	-1318
	ribonuclease III	0.004	-12.77
	ferrochelatase	0.006	-12.31
	gamma-hemolysin component C	0.039	-8.88
	accessory gene regulator protein D	0.043	-8.65
	site specific recombinase	0.046	-8.49
	iron uptake regulatory protein	0.048	-8.39
	competence protein ComGB like protein	0.048	-8.38
SprX1	delta hemolysin	0.002	-15.03
	universal stress protein family protein	0.010	-11.52
	ABC transporter ATP-binding protein	0.011	-11.33
	cell division protein FtsZ	0.018	-10.48
	spermidine/putrescine ABC transporter binding protein	0.022	-10.08
	cobalamin synthesis protein	0.030	-9.48
	SpoU rRNA methylase family protein	0.034	-9.2
	ATL autolysin transcriptional regulator	0.049	-8.33
	N-acetylmuramic acid-6-phosphate etherase	0.049	-8.33
	transcriptional regulator AraC family protein	0.050	-8.29
	immunoglobulin binding protein	z score-1.72	-11.54
	staphylocoagulase	z score 0.22	-7.41
	clumping factorB	z score 0.46	-6.90
	staphylokinase	z score 1.18	-5.35
	immunodominant antigen A	z score 1.93	-3.77
SprX2	delta hemolysin	0.002	-15.03
	iron uptake regulatory protein	0.000	-15.43
	ABC transporter ATP binding protein	0.008	-11.93
	universal stress protein family protein	0.010	-11.5
	transcriptional antiterminator BglG family protein	0.016	-10.75
	cell division protein FtsZ	0.018	-10.48
	serine protease SplD	0.020	-10.32
	enterotoxin family protein	0.024	-9.93
	cobalamin synthesis protein	0.030	-9.48
	SpoU rRNA methylase family protein	0.034	-9.2
	transcription elongation factor NusA	0.039	-8.88
	transcriptional regulator AraC family protein	0.050	-8.29

	clumping factorB	z score-1.59	-12.31
	staphylocoagulase	z score-0.44	-9.66
	immunodominant antigen A	z score-0.27	-9.26
	immunoglobulin binding protein	z score0.16	-8.26
	staphylokinase	z score 0.9	-6.54
SprX3	delta hemolysin	0.002	-15.03
	iron uptake regulatory protein	0.000	-15.43
	ABC transporter ATP binding protein	0.008	-11.93
	universal stress protein family protein	0.010	-11.5
	transcriptional antiterminator BglG family protein	0.016	-10.75
	cell division protein FtsZ	0.018	-10.48
	serine protease SplD	0.020	-10.32
	enterotoxin family protein	0.024	-9.93
	cobalamin synthesis protein	0.030	-9.48
	SpoU rRNA methylase family protein	0.034	-9.2
	transcription elongation factor NusA	0.039	-8.88
	transcriptional regulator AraC family protein	0.050	-8.29
	clumping factorB	z score-1.59	-12.31
	staphylocoagulase	z score-0.44	-9.66
	immunodominant antigen A	z score-0.27	-9.26
	immunoglobulin binding protein	z score0.16	-8.26
	staphylokinase	z score 0.9	-6.54
SprF1	hypothetical protein	0.000	-18.24
	C-terminal part of fibronectin binding protein B	0.006	-12.31
	C-terminal part of fibronectin binding proteinA	0.006	-12.31
	transcriptional regulator DegU family protein	0.012	-11.2
	hydrolase, haloacid dehalogenase like protein	0.016	-10.77
	MutT domain-containing protein	0.022	-10.09
	ribulose phosphate 3-epimerase	0.023	-10.00
	glycosyl transferase, group 1 family protein	0.035	-9.14
	putative GTP cyclohydrolase	0.037	-9.03
	phosphonates ABC transporter permease	0.037	-9.01
	3-hydroxyacyl-CoA dehydrogenase FadB like protein	0.039	-8.88
SprG1	1. hypothetical protein	0.043	-8.68
	2. acetyl-CoA carboxylase subunit beta	0.047	-8.45
	3. osmotic stress-related protein	0.047	-8.44

The parameters used for prediction includes P-value threshold of ≤0.05, with the hybridization seed of 8 and output displayed here indicates the higher order rank list of the targets.

4.2. SprX- a small noncoding RNA

4.2.1. *in silico* characterization of SprX ncRNA

The ncRNA SprX, approximately 156/154 nt in size encoded in the pathogenicity island of *S. aureus* strain Newman was originally identified in Methicillin Resistance *Staphylococcus aureus* N315 strain (Bohn *et al.*, 2010). SprX is highly conserved among several staphylococcal strains, including *S. aureus* Newman which contains three chromosomal copies (Eyraud *et al.*, 2014) named as SprX1, SprX2, SprX3. SprX1 is flanked by genes encoding staphylokinase and truncated amidase while both SprX2 and SprX3 with 100% sequence similarity are flanked by phage amidase and hypothetical protein (Fig. 14).SprX in N315 encodes a putative polypeptide of 40 amino acids found at the 3' end of the sequence (Bohn *et al.*, 2010). However, due to the variation within SprX nucleotide sequence and by its size in Newman, no possible coding protein was found in strain Newman.

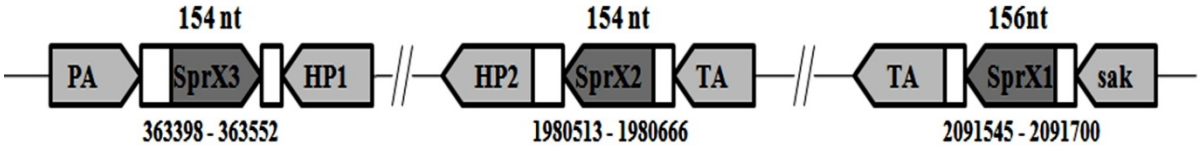

Fig. 14. Schematic representations of the genetic organization of *S. aureus* SprX from strain Newman. The ORFs, orientation of SprX gene and nucleotide (nts) numbers correspond to Newman strain.

The secondary structures of SprX were predicted using online software *mfold* (Fig. 15). SprX1 is characterized by the presence of four stems and SprX2/SprX3 by three stems and U- rich loops.

4.2.1.1. Sequence alignment of Newman SprX with other *S. aureus* strains

Sequence analysis of SprX in Newman was compared with other *S. aureus* strains (Fig. 16) using multiple sequence alignment tool clustalW. The SprX in most of the strains varies in length (149 - 157 nt) with 1 to 2 copies, except *S. aureus* Newman which contain 3 copies. The copy number of the *sprX* gene among the genomic sequences of *S. aureus* strains is listed in Table 16. The sequence variation among the copies of SprX in Newman revealed that 156 nt long SprX1 differs from the 154 nt SprX2 and SprX3 by 6 nt.

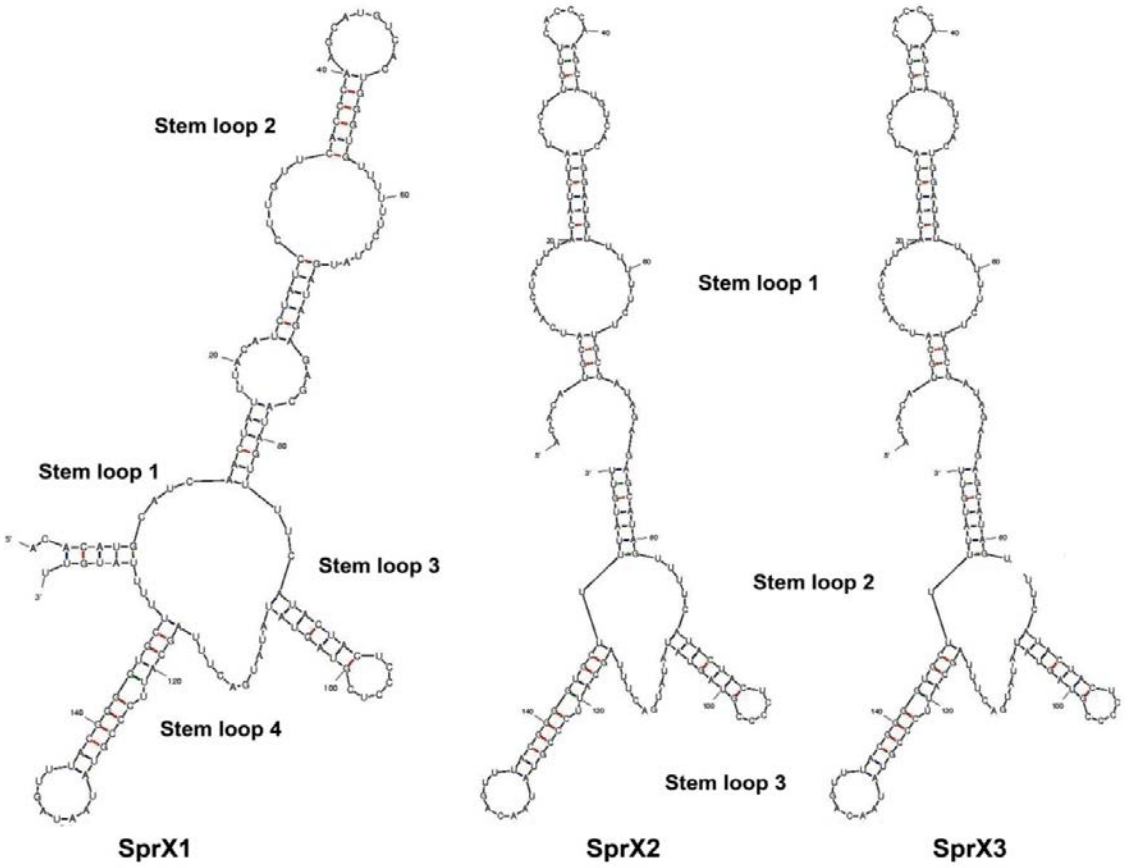

Fig. 15.Secondary structure prediction of SprX by Mfold.

Table 16. The copy number of SprX gene among the genomic sequences of *S. aureus* MRSA and MSSA strains.

***S. aureus* strain**	**Copy number of SprX**
N315	**1**
MRSA 252	**2**
MSSA 476	**1**
Newman	**3**
Mu50	**1**
MW2	**1**
USA 300	**1**
JH1	**1**
JH9	**1**
NCTC 8325	**2**
2395 USA500	**2**
COL	**1**
JKD6008	**2**
ST398	**2**
TW20	**2**
XN108	**2**
HG001	**2**

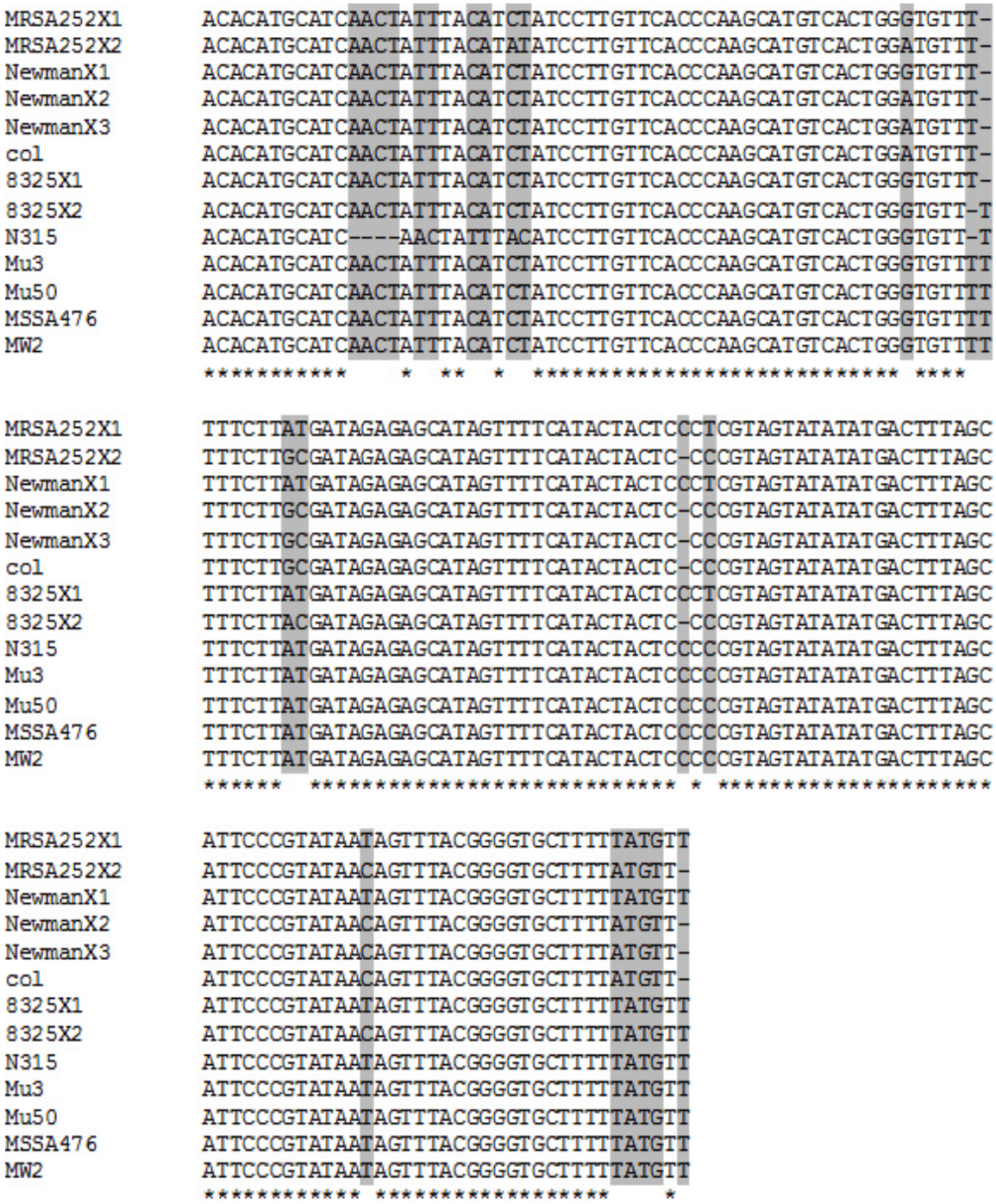

Fig. 16. ClustalW sequence alignment of SprX. Alignment of the nucleotide sequence of SprX from the three SprX copies from *S. aureus* strain Newman compared with other *S. aureus* strains. Identical nucleotides in the sequences are indicated with asterisks*, non identical sequences are highlighted in grey shade.

4.2.1.2. *in silico* predicted mRNA targets of SprX1 selected for this study

Bioinformatic analysis of target prediction tools such as TargetRNA, RNApredator and IntaRNA programs revealed possible interaction of SprX1 with multiple mRNAs as targets. These include the clumping factor B (*clfB*), staphylokinase (*sak*), staphylocoagulase (*coa*), immunoglobulin binding protein (*sbi*), delta hemolysin (*hld*) which were selected for further analysis are given in Table 17.

Table 17. Bioinformatic prediction of targets of SprX1 and their base pairing region.

```
     sRNA 1-33          5′ ACACAUGCAUCAACUAUUUAC-AUC-UAUCCUUGU 3′
                           ||| |: |||||||||||| | ||| :||| :|||
 hld mRNA -25-9         3′ UGU-UGAGUAGUUGAUAAAAGGUAGUGUAGAGACA 5′
     sRNA 53-63         5′ GAGGAAGCGCC 3′
                           ||||||||||
 sak mRNA -10-0         3' CUUUUUUGUGG 5'

     sRNA 42-59         5' GAACACCCAGA-ACGUG 3'
                           ||||||||||  |||||
 sbi mRNA 232- 247      3' UUUGUGGGUCACUGUAC 5'

     sRNA 56-70         5' AUCAUAAAGAAAAAG 3′
                           ||||||| |||||||
clfB mRNA 2723-2738     3′ UAGUAUU-CUUUUUU 5'

     sRNA 45-65         5' AAGAAACAACACAACCA-GUU 3′
                           |||||| |||||  ||| | |
 coa mRNA 1039-1061     3' UUCUUUUUUGUG--GGUCA-C 5'
```

The selected targets for the present study include *clfB, sak, coa, sbi* and *hld* binds to the stem loop 2 of SprX1.Among the selected targets, *sak* gene is present adjacent or flanked by SprX1, where as other target genes are present at distant locations to the SprX1. SprX2 and SprX3 showed weak base pairing region with SprX1 targets *clfB, sak, sbi, coa* in bioinformatic analysis as both the copies differ from SprX1 by 6 nucleotides, due to which they show less efficiency of binding to the mRNA targets of SprX1.

4.2.2. Functional characterization of SprX1

4.2.2.1. Overexpression of SprX1 in *S. aureus* Newman

SprX1 region along with its endogenous promoter was PCR amplified from wild type *S. aureus* Newman (Fig. 18A) (as in materials and methods (Table 9)) cloned in pBluescriptKS^{+} at SmaI site. The recombinant plasmid, pBSprX was confirmed by insert release using BamHI/KpnI (Fig. 18B) and further by DNA sequencing. The insert from

pBSprX clone was subcloned in *E. coli* - Staphylococcal shuttle vector pCN40 in two separate pairs of digestion with SalI/BamHI and BamHI/KpnI to get the gene in both sense and antisense orientation respectively. The obtained clones (Fig. 17) were named as pMNSprX (Fig. 18C) and pMNSprX$_{AS}$ (Fig. 18D).

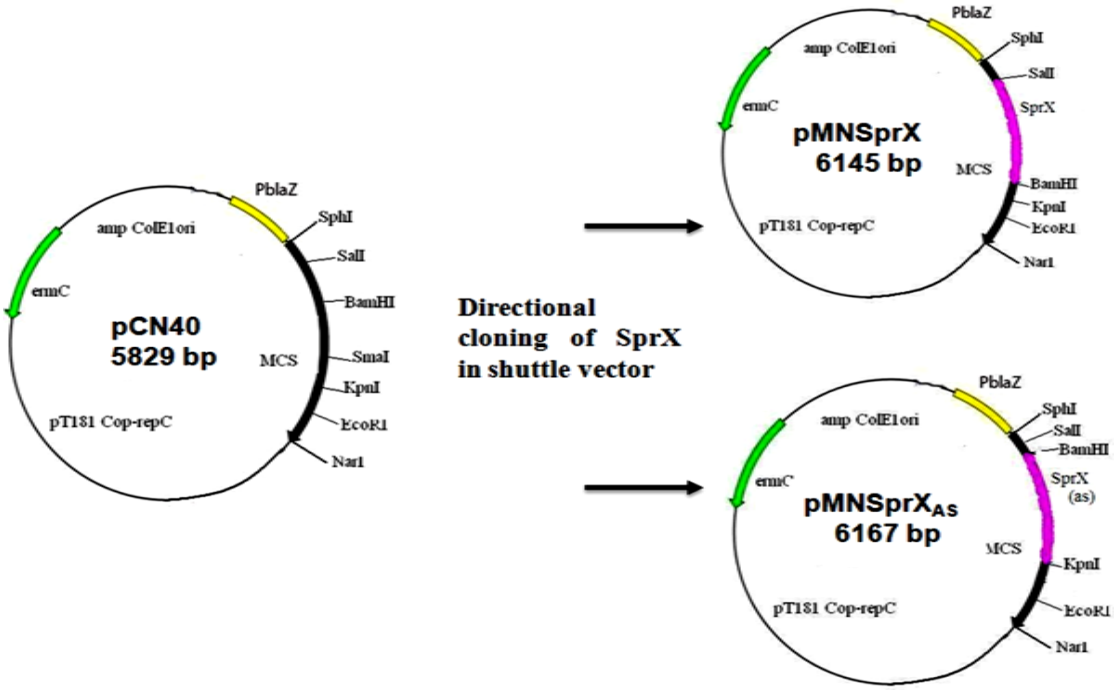

Fig. 17. Schematic representation of cloning of SprX1 in *E. coli* - staphylococcal shuttle vector. SprX was subcloned in pCN40 shuttle vector using the respective enzymes SalI/BamHI and BamHI/KpnI to get the gene in both the orientation. pMNSprX, pMNSprX$_{AS}$: overexpression and antisense constructs of SprX1.

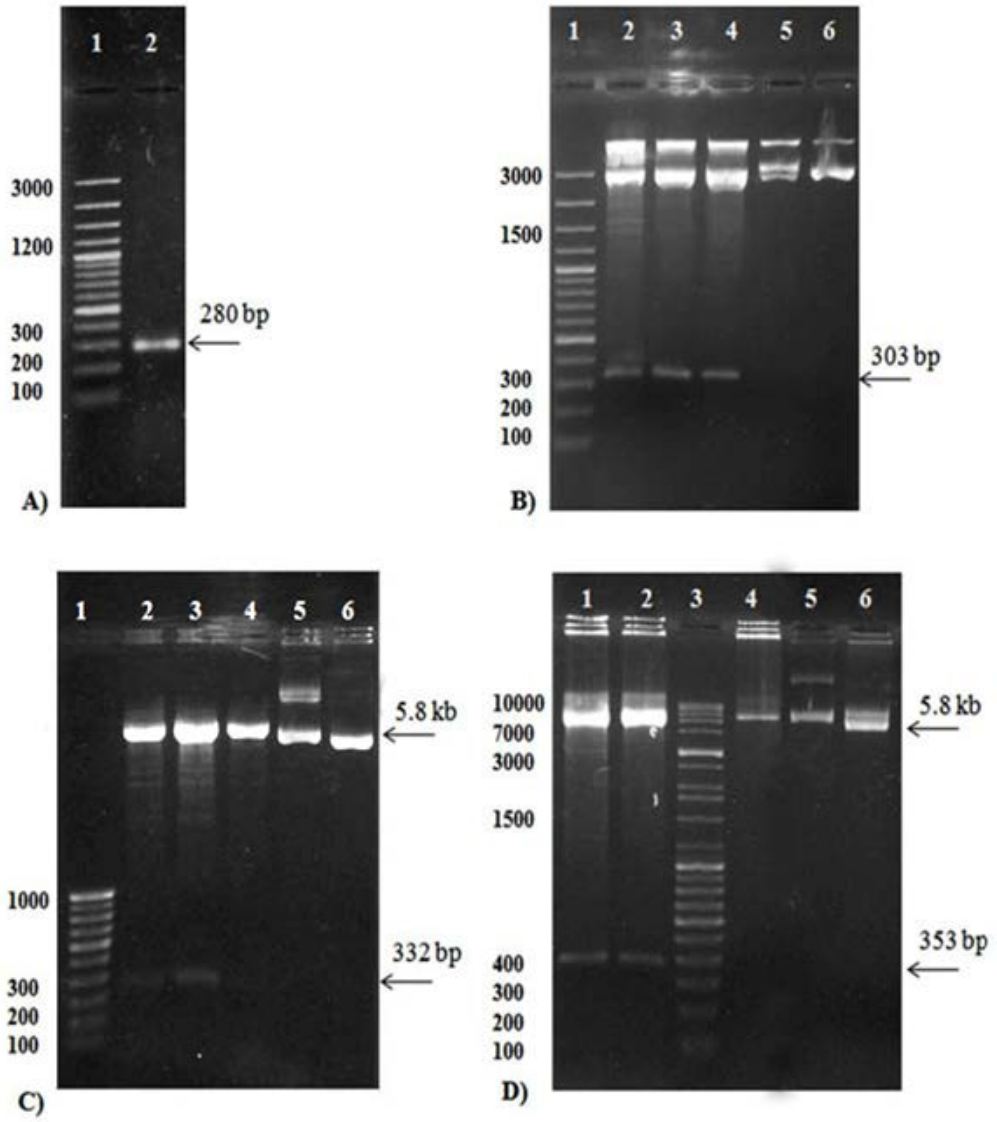

Fig. 18. PCR amplification, cloning and subcloning of SprX1.

A. Lane 1: 100 bp marker (100-3000 bp), Lane 2: SprX1 (280 bp).

B. Lane 1: 100 bp Marker (100-3000 bp), Lane 2,3,4: pBSprX clones digested with BamHI/HindIII showing insert release of 303 bp, Lane 5:Linearization of pBSprX with HindIII, Lane 6: Linearization of pBSKS with HindIII.

C. Lane 1: High range Marker (100-1000 bp), Lane 2,3: pMNSprX digested with SalI/BamHI showing insert release of 332 bp, Lane 4: Linearization of pMNSprX with BamHI, Lane 5: undigested pMNSprX, Lane 6: Linearization ofpCN40 with HindIII.

D. Lane 1,2: pMNSprX$_{AS}$ digested with BamHI/KpnI showing insert release of 353 bp, Lane 3: High range Marker (100-10000 bp), Lane 4: Linearization of pMNSprX$_{AS}$ with BamHI, Lane 5: undigested pMNSprX$_{AS}$, Lane 6:Linearization ofpCN40 with BamHI.

All plasmid constructs were created using *E. coli* DH5α as the intermediate host. Newly generated plasmids were confirmed by the restriction digestion patterns and subsequently transformed in *S. aureus* Newman by passaging through intermediate host restriction deficient *S. aureus* RN4220.

4.2.2.2. Disruption of *sprX1* using kanamycin marker

The chromosomal copy of *sprX1* was disrupted by using recombinant plasmid achieved by three step cloning using the following strategy represented diagrammatically in Fig. 19.

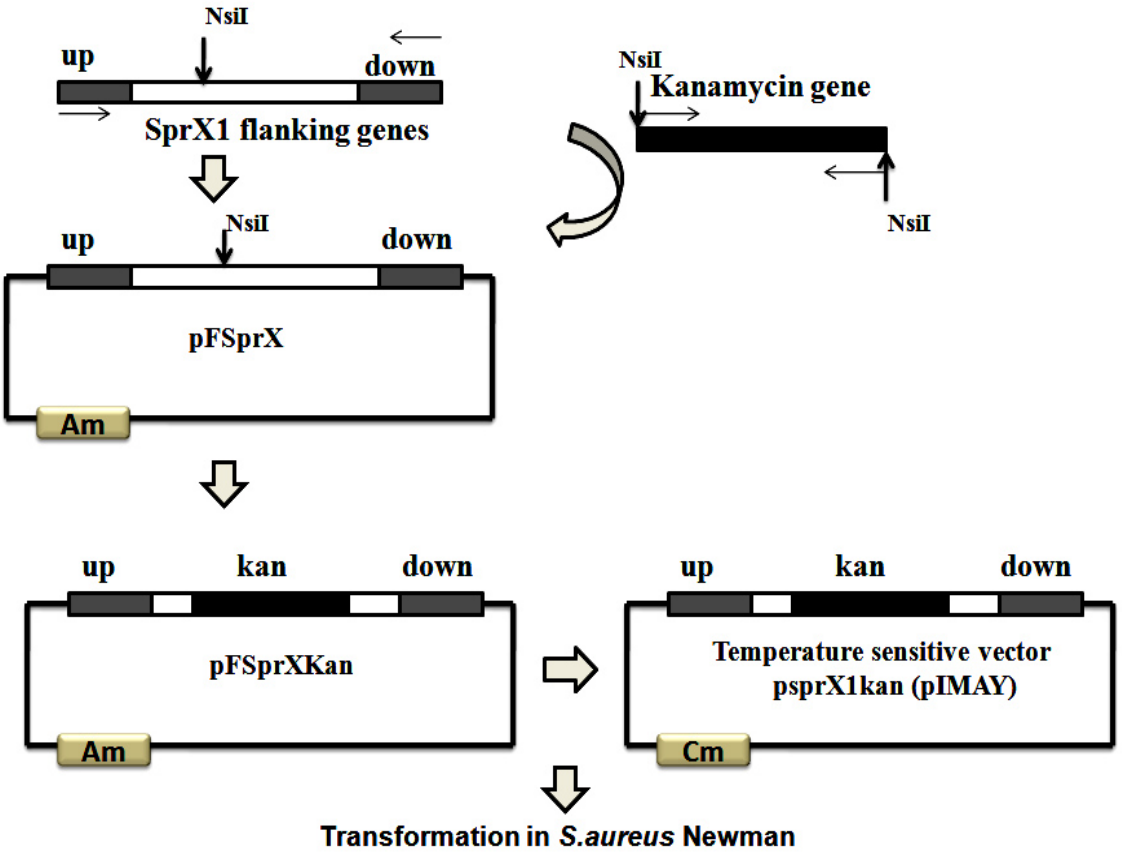

Fig. 19. Schematic representation of cloning strategy of disruption of *sprX1*. *sprX1*gene disruption was achieved by cloning the kanamycin cassette at the NsiI site in pFsprX to yield disrupted cassette of *sprX1::kan* in pFSprXKan and subcloned in temperature sensitive vector (pIMAY) which replicates at 37°C in *E. coli* and 30°C in *S. aureus*.

A 1.5-kb DNA flanking 700 and 800 bp upstream and downstream respectively of SprX1 gene was amplified from *S. aureus* Newman (Fig. 20A) using the primers FsprX1 (F) and FsprX1 (R) (Table 7) and cloned into the SmaI site of pBSKS to

generate pFsprX (Fig. 20B). The *sprX1* gene in the above construct was inactivated by inserting the kanamycin gene at +10 position of SprX1 using NsiI to generate pFsprXKan (Fig. 20C).

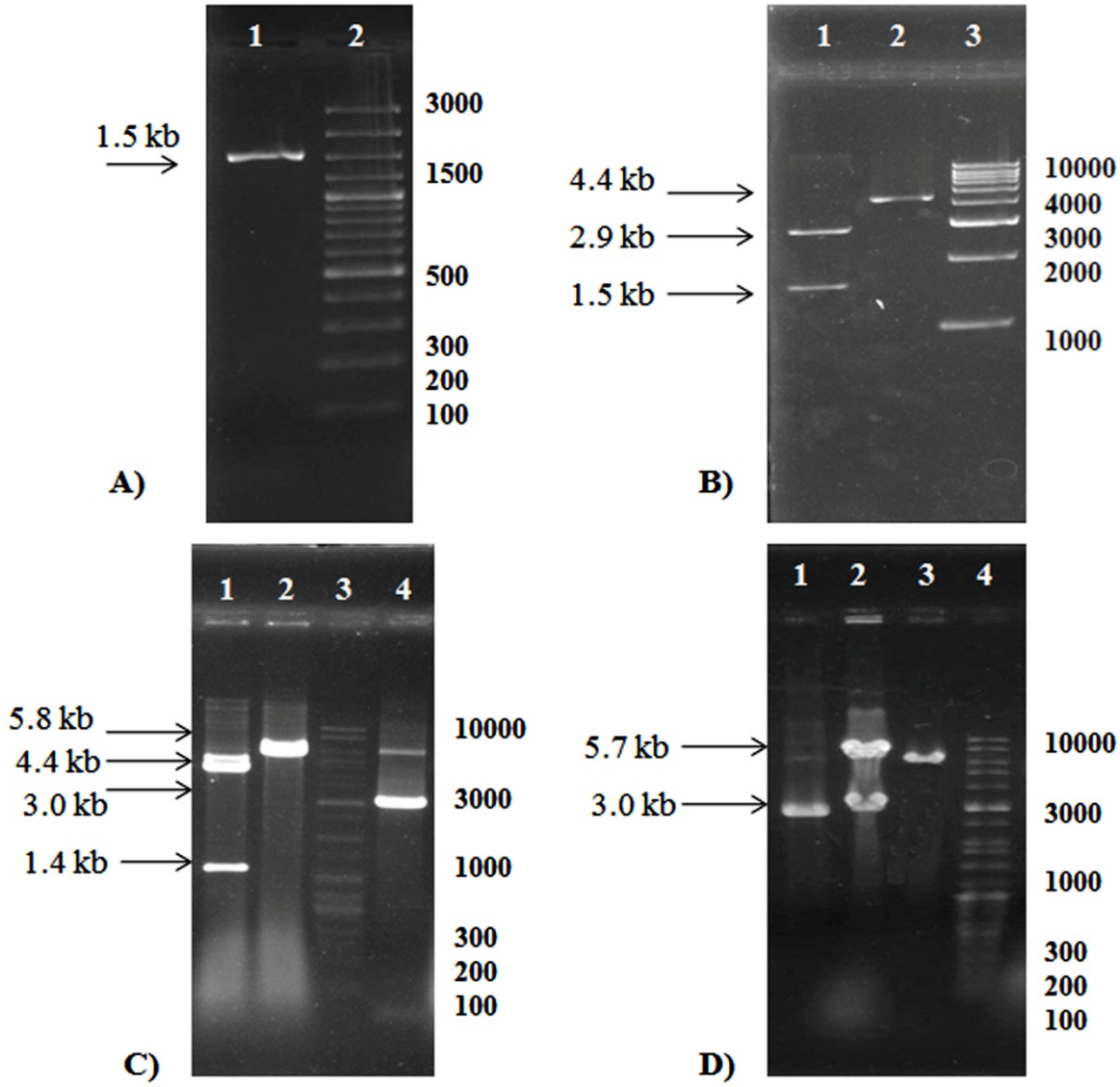

Fig. 20. PCR amplification, cloning and subcloning of gene disruption cassette *sprX1::kan.*

A. Lane 1: Flanking sequence of SprX1 (1.5 kb), Lane 2: Medium range marker (100-5000 bp).
B. Lane 1: pFsprX digested with BamHI and KpnI showing insert release of 1.5 kb, Lane 2: Linearization of pFsprX with PstI (4.4 kb), Lane 3: 1 kb DNA ladder (1000-10000 bp).
C. Lane 1: pFsprXKan digested with NsiI showing insert release of kan (1.4 kb), Lane 2: Linearization of pFsprXKan with HincII (5.8 kb), Lane 3: High range marker (100-10000 bp), Lane 4: PCR amplification of disrupted cassette *sprX::kan* from pFsprXKan (2.9 kb).
D. Lane 1: PCR amplification of disrupted cassette *sprX1::kan* from psprX1kan (2.9 kb), Lane 2: psprX1kan digested with BamHI showing insert release of 2.9 kb, Lane 3: Linearization of pIMAY with BamHI (5.7 kb), Lane 4: High range marker (100-10000 bp).

The disrupted *sprX1::kan* fragment was cloned into the BamHI site of the temperature sensitive plasmid pIMAY to generate the disruption plasmid psprX1kan (Fig. 20D) and was passed through methylation defective mutant *E. coli* strain DC10B before electroporation into *S. aureus* Newman. Transformants were selected on double antibiotic chloramphenicol and kanamycin plate at the permissive temperature 30°C. *sprX1* chromosomal gene disruption in *S. aureus* Newman was achieved by homologous recombination at the flanking sequence at nonpermissive temperature of 37°C (Monk *et al.*, 2012) and putative mutants were analyzed and confirmed by PCR, Northern and Southern analyses. Further, the disruption strain was complemented with SprX1 overexpression plasmid for restoration.

4.2.2.3. Expression analysis of altered level of SprX constructs

4.2.2.3.1. Analysis of SprX1 overexpression by Northern blot

The expression of altered level of SprX1 in the modified strains of *S. aureus* Newman was analysed by hybridization of total RNA with strand specific DIG-labelled SprX riboprobes.

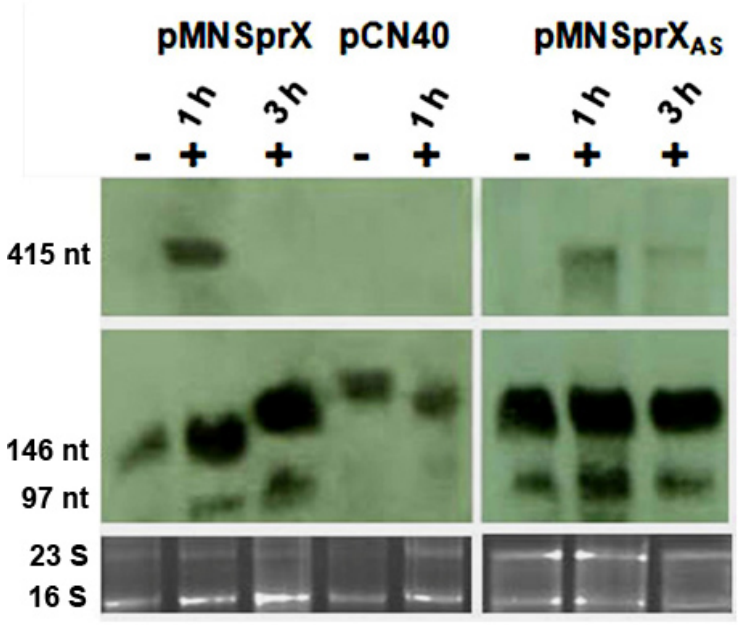

Fig. 21. Expression analysis of SprX1 by Northern blot. Total RNA isolated from *S. aureus* Newman strains bearing the overexpression, pCN40 and antisense of SprX1 was hybridized with strand specific DIG-labeled SprX1 RNA probes. pMNSprX, pCN40, pMNSprX$_{AS}$: overexpression, control vector and antisense SprX. -/+ indicates uninduced and induced with 0.5 µg/ml of methicillin. Loading control shown are 23S and 16S rRNA.

The cultures were induced with 0.5 µg/ml of methicillin at the OD_{600} 4.0 to drive the expression of cloned SprX1 under the *blaZ* promoter in the shuttle vector pCN40 at two different time intervals, 1 and 3 h. Northern blot analysis indicated two kinds of transcripts, the one expressed from the endogenous promoter of SprX1 and the other expressed from the *blaZ* promoter. Maximum expression was seen from endogenous promoter which produced 146 nt SprX1 transcripts while poor expression of a 415 nt long transcript was seen from PblaZ (Fig. 21), in stationary phase cultures. Although, the poor expression of SprX1 from *blaZ* promoter in the overexpression construct was not anticipated, higher expression of the intact RNA from the endogenous promoter in the multi-copy clone resulted in sufficient fold increase to make comparisons. The construct expressing antisense SprX from PblaZ also revealed the SprX1 transcripts, probably originating from its own inherent promoter. Strain bearing vector pCN40 served as the control.

4.2.2.3.2. Analysis of *sprX1* disruption mutant by PCR, Northern and Southern blot

Chromosomal copy of *sprX1* was disrupted by inserting kanamycin resistance gene close to the promoter region of SprX1 by homologous recombination. The expression of *sprX1* in the disrupted mutant was confirmed by Northern blot, by isolating the total RNA of both the disruption and wild type Newman strain and hybridized with DIG-labeled SprX probe. The result indicated the absence of expression of *sprX1*, although both the wild type and disruption strain expressed an additional 100 nt transcript of size which could have arisen from the additional gene copies of *sprX* shown in Fig. 22A.

Further, the chromosomally disrupted *sprX1* in *S. aureus* Newman was confirmed by PCR using the ncRNA primers SprX1 and flanking region of SprX1 forward and reverse primers respectively which yielded higher amplification of 1.6 and 2.9 kb in the disruption strain when compared to the wild type Newman shown in Fig. 22B.

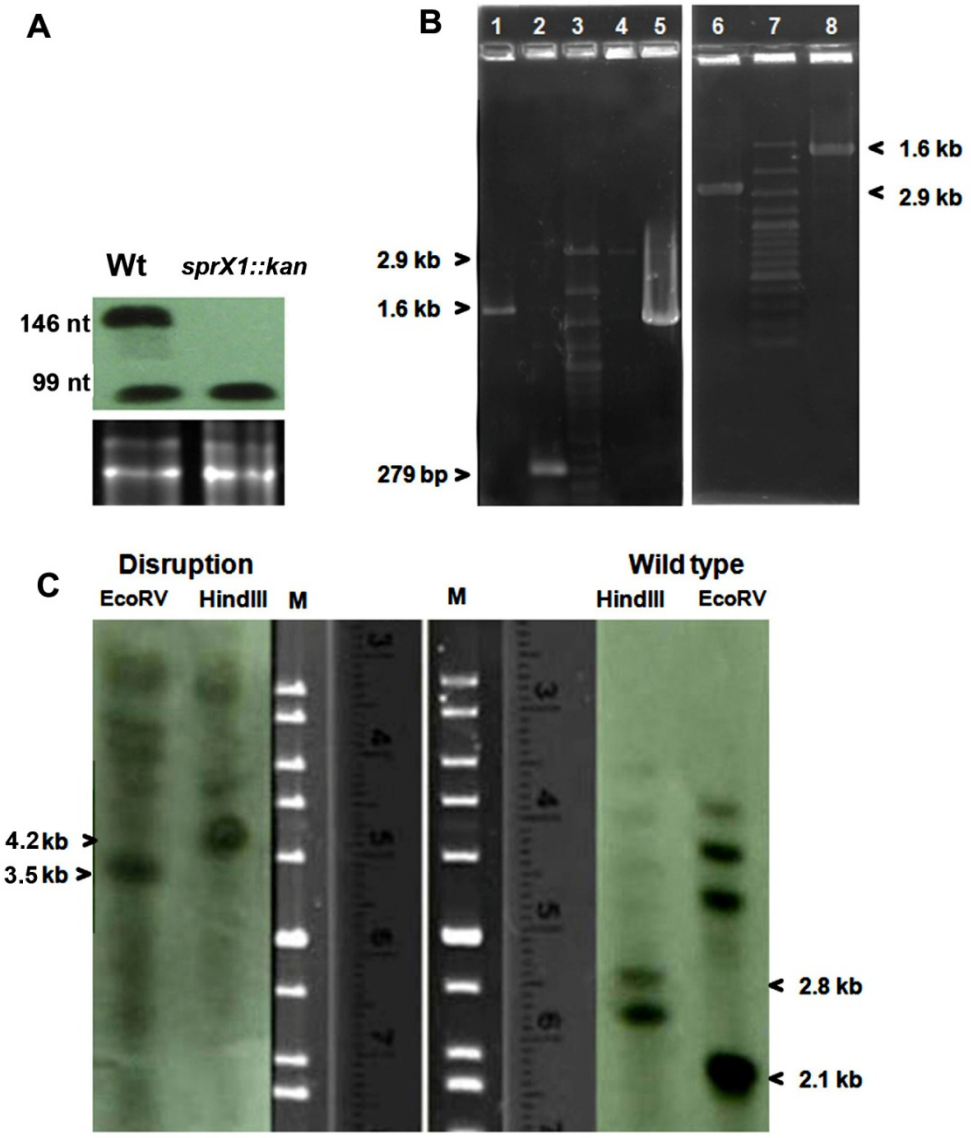

Fig. 22. Confirmation of disruption mutant *sprX1::kan* strain.

A. Northern blot analysis of SprX expression. Total RNA from *S. aureussprX1::kan* and wild type Newman strain hybridized with DIG-labeled SprX. Loading control shown are 23S and 16S rRNA at the bottom of the gel.

B. Analysis of disruption strain by PCR using primers of SprX1 and flanking sequence. Lane 1, 4: chromosomal *sprX1::kan*, Lane 2, 5: wild type Newman, Lane 6, 8: Positive control plasmid psprX1kan, all were amplified with SprX1 primers or flanking SprX sequence primers respectively, Lane 3, 7: indicates marker ranging from 100 to 3000 bp.

C. Southern blot analysis of *sprX1* disruption and the isogenic wild type *S. aureus* Newman. Genomic DNA was digested with HindIII and EcoRV and hybridized with SprX probe. The chromosomal disruption of *sprX1* was indicated by an increase of 1.4 kb (4.2 kb, 3.5 kb) in the molecular weight of bands 2.8, 2.1 kb of the wild type digested with HindIII and EcoRV respectively. The presence of additional bands is attributed to partial digestion by the enzymes. M- Marker, 100 to 10000 bp.

Table 18. Digestive band pattern of genomic loci of *sprX* in *S. aureus* Newman and disrupted strain.

Copy	Wild type (in bp)		Disruption (in bp)	
	HindIII	EcoRV	HindIII	EcoRV
SprX1	2860	2154	4260	3554
SprX2	5336	3865		
SprX3	6202	4591		

S. aureus Newman DNA sequence analysis for HindIII and EcoRV restriction enzymes at the loci of three SprX copies indicated bands of molecular size as in Table 18 Genomic DNA from the s*prX*1 disruption and its isogenic strain was digested with both of the restriction enzyme and probed with SprX1. The disruption mutant selected showed insertions in SprX1 as indicated by an increase of 1.4 kb molecular weight in attributed to kanamycin insertion. Hybridization band pattern was in agreement with the disruption of *sprX1* shown in Fig. 22C. The presence of additional bands could be attributed to partial digestion by these enzymes.

4.2.2.4. Effects of altered expression of SprX1 on various pathogenecity factors

4.2.2.4.1. Effect of SprX1 on growth physiology

Whether the modulated expression of SprX1 in the clinical isolate *S. aureus* Newman has any adverse effect on the growth physiology of the organism, the growth rate of the strain bearing overexpression of SprX1, knockdown (antisense of SprX1) and disruption of *sprX1* with the comparison of the vector control was studied at OD_{600}. Overexpression of SprX1 had no major consequence on the growth rate of *S. aureus*, however, the strain bearing a disrupted *sprX1* strain displayed reduced growth rate (Fig. 23). This suggests that SprX1 may act as a common regulator, when it is disrupted it might affect the several downstream genes such as cell division proteins which are essential for the normal functioning of the cell. All the experimental datas were normalised for mg/ml cell protein to account for the difference in the growth rates. 5S rRNA was used as internal control in real time PCRs.

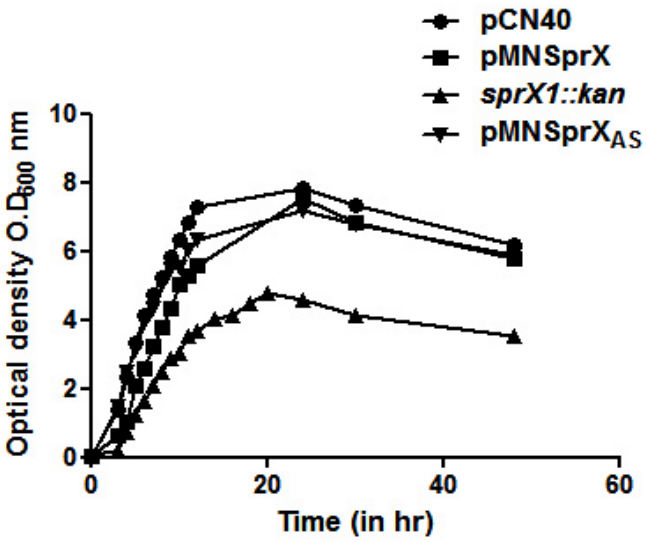

Fig. 23. Growth physiology of altered strains of *S. aureus* Newman expressing SprX1. *S. aureus* Newman bearing pCN40 (vector control), pMNSprX (overexpression), *sprX1::kan* (disruption) and pMNSprX$_{AS}$ (antisense).

4.2.2.4.2. Influence of SprX1 on staphylococcal delta hemolysin

Staphylococcal delta hemolysin, a 26 amino acid extracellular cytotoxin differs from other hemolysins such as alpha, beta and gamma by its heat stable nature and its activity on erythrocytes of various species. It affects the variety of cell types including human neutrophils, monocytes, T-cells and causes oxidative burst, release of inflammatory cytokines, inhibits water absorption and activates adenylate cyclase in the ileum, inhibits the binding of epidermal growth factor to the cell surface receptors (Schmitz *et al.*, 1997). Delta hemolysin (*hld*), produced at the late exponential phase, is transcribed within another regulatory small RNA, RNAIII, was identified as one of the targets for SprX1. *in silico* analysis indicated that SprX1 interacts with 26 nucleotides in the 5' untranslated region (UTR) including the shine Dalgarno sequence and AUG codon of the mRNA encoding delta hemolysin.

Overexpression of SprX1 resulted in a 1.5- fold increase of Hld mRNA in real time PCRs whereas it was downregulated in the disruption strain (Fig. 24). The increase in Hld transcripts was also paralleled by a 72% increase in hemolysis of human RBC (Fig. 25A). A primer pair corresponding to Hld mRNA and 3' end of RNAIII (Table 7) was used for their simultaneous and coupled detection. This increase in RNAIII was also reflected by a 32% increase in the activity of alpha hemolysin (Fig. 25B) which is one of its well studied targets (Morfeldt *et al.*, 1995). The increased alpha hemolysis on rabbit

RBCs is an indirect evidence for the stability of RNAIII transcripts in the presence of SprX1. Complementation of overexpression plasmid pMNSprX in *sprX1* disruption mutant strain also resulted in restoration of delta and alpha hemolysis activities (Fig. 25A and Fig. 25B).

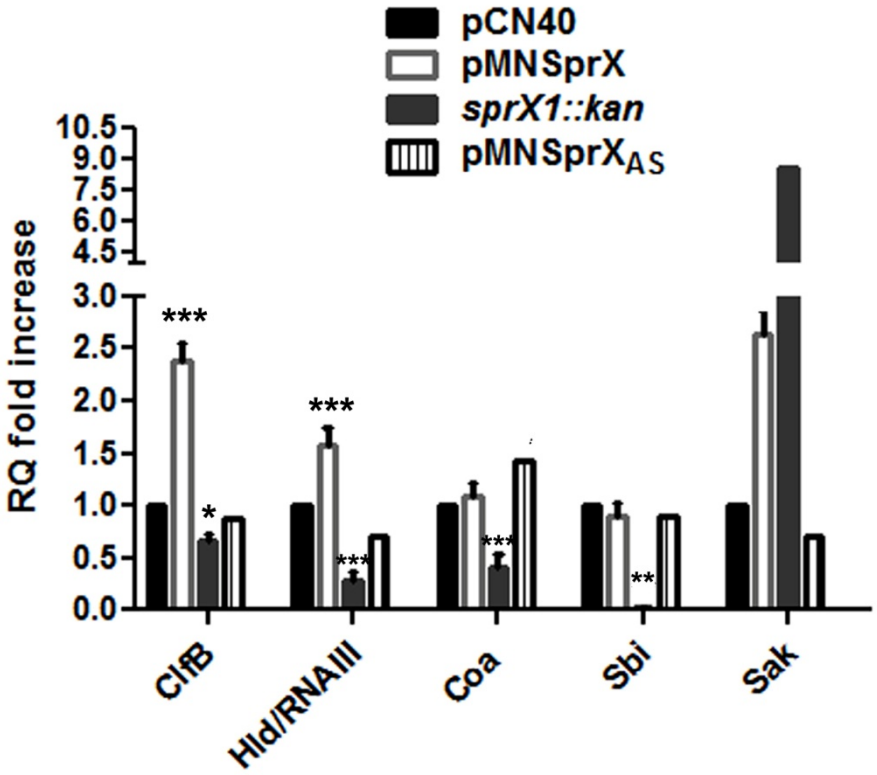

Fig. 24. Expression of predicted targets under altered levels of SprX1 in *S. aureus* Newman. qRT-PCR analysis of expression of target genes in control (pCN40), SprX1 overexpression (pMNSprX), disruption (*sprX1::kan*) and pMNSprX$_{AS}$ (antisense) constructs. *clfB* - clumping factor B, *hld/RNAIII* - delta hemolysin, *coa* - staphylocoagulase, *sbi* - immunoglobulin binding protein and *sak* - staphylokinase. Asterisks represent significant statistical differences determined for each of the genes compared with the vector control by using two way ANOVA ***($P < 0.001$), *($P < 0.05$) and **($P < 0.01$). 5S rRNA was used as an endogenous control.

SprX1 may exert its effect in influencing both Hld and RNAIII levels. It is reported that intramolecular base pairing of 5' and 3' end of RNAIII blocks the ribosomal binding site of Hld mRNA (Benito *et al.*, 2000). The interaction of SprX1 with the RNAIII in this region possibly may release this intramolecular base pairing leading to changes in the secondary structure and allowing the ribosome to bind for effective translation.

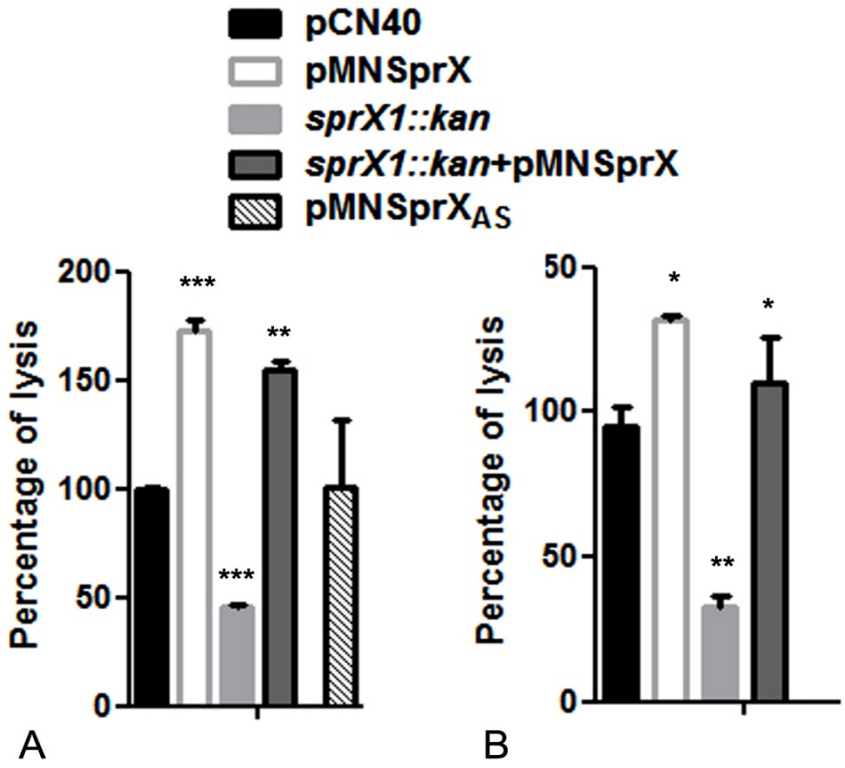

Fig. 25. Spectrophotometric assay of A) delta hemolysis and B) alpha hemolysis. Culture supernatant of *S. aureus* Newman strains incubated with human RBCs and rabbit RBCs and measured the $OD_{541/416}$ nm respectively. pCN40 (vector control), pMNSprX (SprX overexpression), *sprX1::kan* (disruption), *sprX1::kan* + pMNSprX (complementation) and $pMNSprX_{AS}$ (antisense). Asterisks represent the significant statistical differences of $P \leq 0.0001$ and $P \leq 0.0014$ respectively for A and B when each construct was compared with the vector control as determined by one way ANOVA.

The potential interaction of SprX1/Hld was also verified by *in vitro* gel mobility shift assay (discussed below). These results combined with bioinformatic analysis indicate the positive modulation of hemolysin expression by SprX1.

4.2.2.4.3. SprX1 plays a significant role in biofilm formation

One of the major defense mechanism of *Staphylococcus aureus* is the capacity to form biofilms. Biofilm formation often occurs on medical devices, like catheters and heart valves, which are in direct contact with blood. Biofilm formation is a complex process stimulated by multiple factors including external environment such as extracellular DNA (eDNA), DNase, biomolecules and as well as internal stimuli of an organism (Archer *et al.,* 2011). Biofilm formation by pathogenic strains of *S. aureus* is paralleled with differential expression of a number of genes leading to invasiveness and persistent infection (Resch *et al.,* 2005). Several functionally diverse proteins such as ClfB,

glucosaminidase, IsdA, IsaA, SACOL0688 and nuclease have been detected in biofilms of *S. aureus* strains (Den Reijer *et al.*, 2016).

Clumping factor B (ClfB), one of the mediators of PIA (Polysaccharide intercellular adhesin) independent biofilm formation (Kirmusaoglu, 2016), was revealed as one of the targets of SprX1 in the target prediction tools. A 14 nucleotide stretch within the 3' coding region of clumping factor B mRNA showed potential base pairing with SprX1. The expression of *clfB* exhibited 2.24- fold increased levels under the overexpression of SprX1 while it was 0.7- fold of the control when the chromosomal *sprX1* was disrupted, as quantified by real time PCR (Fig. 24). Further, the increase in clumping factor B was in co-relation by a 40% enhancement in the levels of biofilm formation by microtiter plate assay (Fig. 26). In addition to clumping factorB, the glucose induced, PIA dependent biofilm (Kirmusaoglu, 2016; Zmantar *et al.*, 2010) was increased by 40 % by pMNSprX.

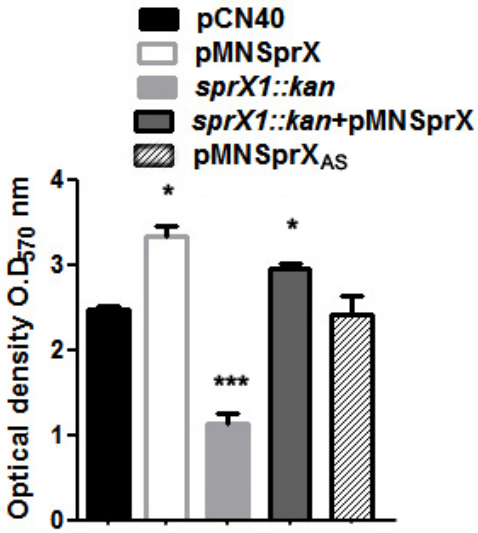

Fig. 26. Influence of SprX1 on glucose induced biofilm formation. Microtiter plate assay of PIA dependent biofilm formation (Zmantar *et al.*, 2010) of different constructs of SprX in *S. aureus* Newman with pCN40 (vector control), pMNSprX (overexpression), *sprX1::kan* (disruption), *sprX1::kan*+pMNSprX (complementation) and pMNSprX$_{AS}$ (antisense). Statistical difference *($P \leq 0.0001$) between the constructs was determined by using one way ANOVA on comparison with the vector control.

Complementation by SprX1 partly restored the biofilm in the *sprX1* disruption strain. This relative increase in ClfB, which is required in the early phase of staphylococcal dissemination in the host (Wertheim *et al.*, 2008; Cheng *et al.*, 2009) suggests that SprX1 may support colonization of *S. aureus* during infection. The RNA-RNA interaction demonstrated association of SprX1 with ClfB is discussed below.

4.2.2.4.3.1. Imaging of increased adherence of biofilm and clumping of cells

The cells overexpressing SprX1 exhibited an increased adherence resulting in a dramatic increase in the biofilm formation, when tested on the glass cover slip, in comparison with the non-homogenous film formed by the disruption, knockdown and control vector strain (Fig. 27 A1, B1, C1, D1). Further, confocal microscopy after FITC staining of planktonic culture grown in 2% glucose demonstrated aggregates of each 4-8 cells as compared to the strain bearing disruption or the control, both of which had uniformly dispersed single cells (Fig. 27, A2, B2, C2, D2). Collectively, these results indicate that increased dose of SprX1 contributes the cell to cell interaction leading to intercellular aggregation and biofilm phenotype. Thus SprX1 is believed to support colonization of *S. aureus* infection via clumping factor B (ClfB), an MSCRAMM (microbial surface components recognizing adhesive matrix molecules) whose expression *in vitro* is several fold higher during the bacterial growth.

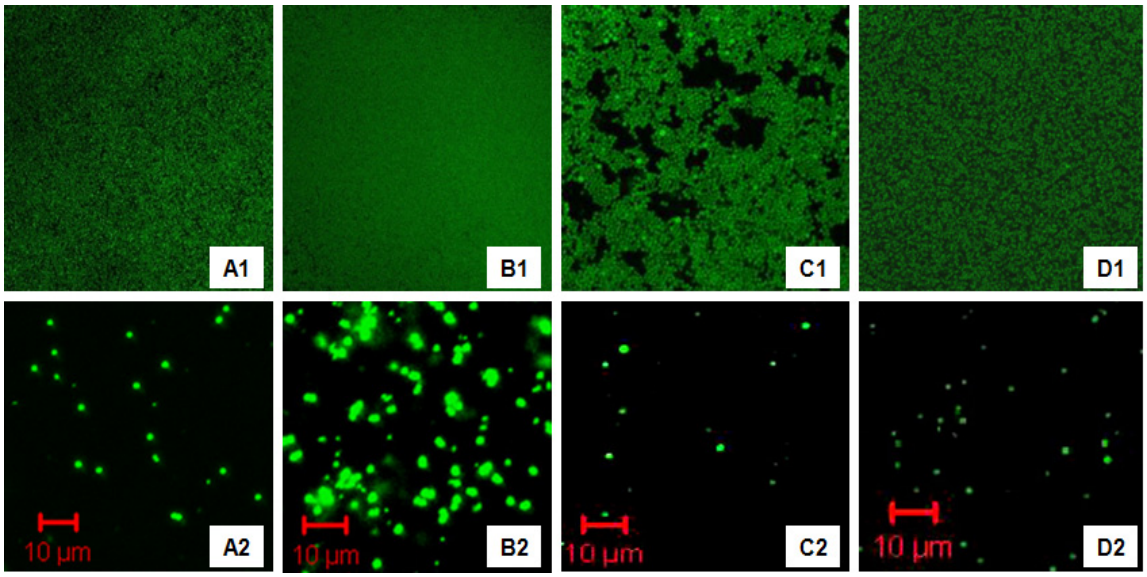

Fig. 27. Confocal laser scanning microscope (CLSM) images of biofilms and clumped cells labelled with Fluorescein isothiocyanate (FITC). Series 1 in upper panels show the biofilm formation on the cover glass slip. Series 2 in lower panels illustrate the clumping of cells in culture suspension of different constructs A) control (pCN40) B) SprX1 overexpression (pMNSprX) and C) disruption (*sprX1::kan*) and D) antisense (pMNSprX$_{AS}$) of *S. aureus* Newman respectively.

SprX1 reported here, is the third sRNA to be involved in biofilm formation in addition to RsaA (Romilly *et al.*, 2014) and RNAIII (Chambers & Sauer, 2013; Coelho *et al.*, 2008; Le and Otto, 2015) in *S. aureus*. The biofilm formation is also associated with genes involved in carbohydrate metabolism including those involved in TCA cycle such as

citB and *citZ* and also other downstream genes such as *ccpA, agr, sarA* (Seidl *et al.*, 2008; O'Gara, 2007).Biofilm formation is known to help the bacterium to circumvent host immune response and protect them from phagocytosis (Thurlow *et al.*, 2011). Several small RNAs such as OmrA/B, Qrr1-4, ArcZ, PhrS have been reported to be involved in biofilm formation and mediating the switch of planktonic cells to surface mediated growth (Chambers & Sauer, 2013)in *E. coli*, *V. cholera, S. typhimurium*, *P. aeruginosa* respectively. It is really interesting to look, how SprX influences the regulation of another noncoding RNA such as RNAIII which is involved in the expression of several virulent targets.

4.2.2.4.4. Other predicted targets of SprX1

Although, the immunoglobulin binding protein (Sbi) staphylocoagulase (Coa) and staphylokinase (Sak) were among the bioinformatically predicted targets (Table 17), there was no correlation in their expression with respect to SprX1 levels. They did not show significant correlation in expression levels in real time PCRs (Fig. 24) under the overexpression of SprX1 as compared to the vector control. However, the downregulation of these genes was observed under the disruption of *sprX1*.These may not be the direct targets for sRNA SprX1 and are being regulated by other regulatory factors. In contrast, the upregulation of *sak* mRNA levels by 3.6- and 8.2- fold increase in both SprX1 overexpression and disruption strains respectively as compared to the vector control in real time PCRs (Fig. 24).

4.2.3. Electrophoretic gel mobility shift assay

The studies on specific interactions of sRNA with target mRNAs of delta hemolysin and clumping factor B by gel mobility shift assay revealed that SprX1 directly base pairs with these virulent mRNAs and regulates them.

4.2.3.1. Generation of SprX1 template by PCR

DNA template SprX1 (150 bp)was generated by PCR from the clone pBSprX using SprX1 primers in which the left primer was tagged with T3 promoter sequence (Table 7 and Table 9) and used as a template for *in vitro* transcription (Fig. 28).

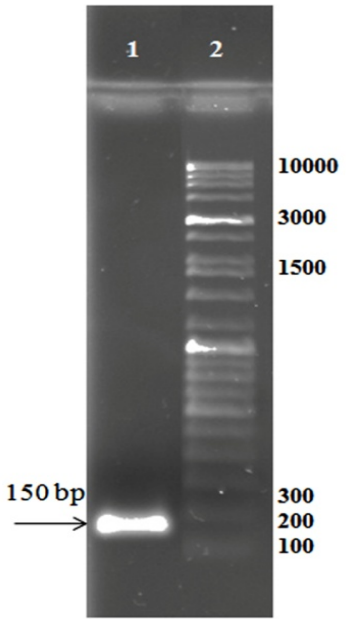

Fig. 28. PCR amplification of SprX1 using pBSprX as template. Lane 1: SprX1 (150 bp), Lane 2: High range marker (100-10000 bp).

4.2.3.2. Cloning of interaction region of delta hemolysin, clumping factor B and PhrD in pBSKS$^+$

DNA fragment spanning the region of -48 to +130 of delta hemolysin (Hld) and +2603 to 2758 of clumping factor (ClfB*)* were generated by PCR using *S. aureus* Newman genomic DNA as template using the hld and clfB primers respectively (Table 7 and Table 9). PCR amplified Hld and ClfB of 179 and 155 bp in size respectively was cloned in pBSKS$^+$ at EcoRV site. Recombinant plasmids, pBShld and pBSclfB were confirmed by restriction digestion (Fig. 29 and Fig. 30) and further by DNA sequencing. Unrelated, non specific competitor *phrD* gene from *P. aeruginosa* was used for competition assays. Recombinant clone pBSPhrD obtained from the lab source, was generated by cloning in pBSKS$^+$ using PstI/XbaI and sequenced.

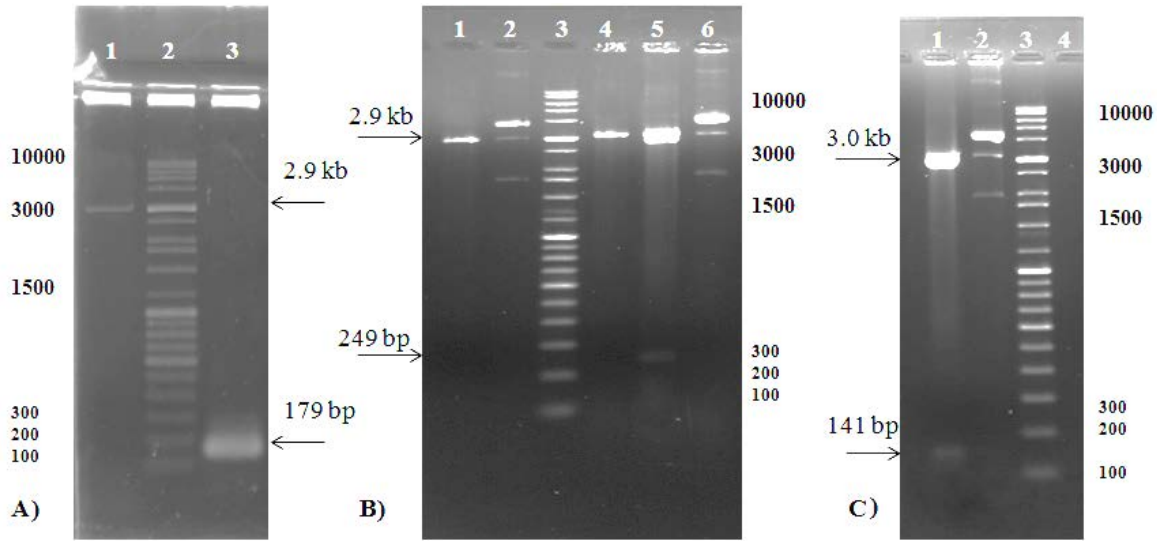

Fig. 29. PCR amplification and cloning of interaction region of delta hemolysin (Hld) in pBSKS^{+}.

A. Lane 1: pBSKS digested with EcoRV, Lane 2: Marker, Lane 3: hld (179 bp).
B. Lane 1: pBSKS digested with KpnI, Lane 2: undigested pBSKS, Lane 3: Marker, Lane 4: Linearization of pBShld with KpnI, Lane 5: pBShld digested with BamHI/KpnI showing insert release of 249 bp, Lane 6: Undigested pBShld.
C. Lane 1: clone pBShld digested with EcoRV/BamHI showing band pattern of 3.0 kb and 141 bp, Lane 2: Undigested pBShld, Lane 3: Marker (DNA marker ranges from 100-10000 bp).

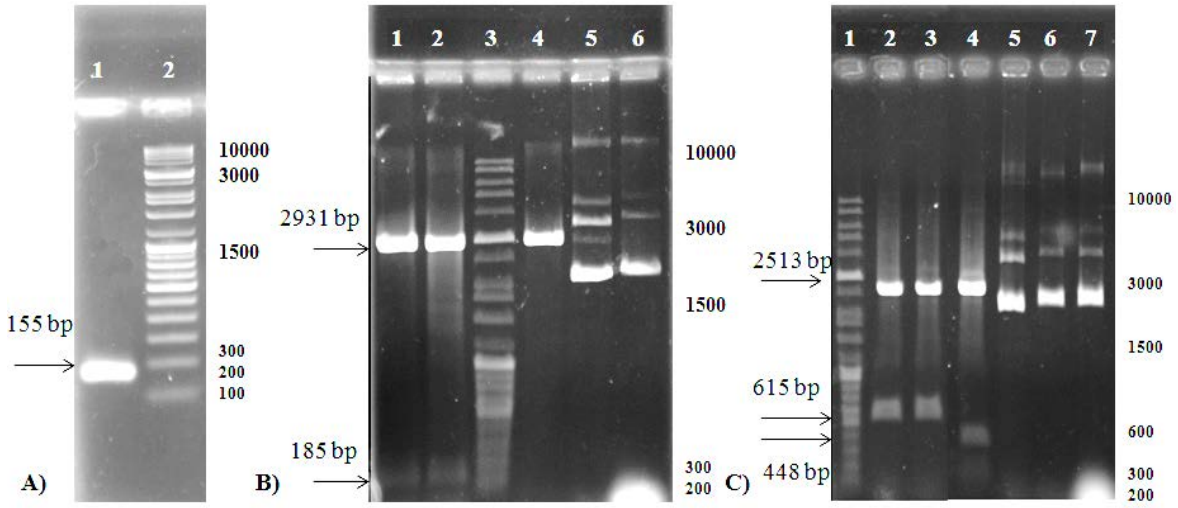

Fig. 30. PCR amplification and cloning of interaction region of clumping factorB (ClfB) in pBSKS^{+}.

A. Lane 1: ClfB (155 bp), Lane 2: Marker.
B. Lane 1 and 2: pBSclfB clones digested with BamHI/HindIII showing insert release of 185 bp, Lane 3: Marker, Lane 4: Linearization of pBSKS with BamHI, Lane 5: Undigested pBSKS, Lane 6: Undigested pBSclfB.
C. Lane 1: Marker, Lane 2 and 3: pBSclfB clones digested with PvuII showing 2.5 kb and 615 bp bands, Lane 4: pBSKS digested with PvuII showing 2.5 kb and 448 bp bands, Lane 5: Undigested pBSKS, Lane 6 and 7: Undigested pBSclfB clones (DNA marker ranges from 100-10000 bp).

4.2.3.3. *in vitro* sRNA-mRNA interaction assay

The interaction of computationally predicted specific target sequences in Hld and ClfB mRNAs with SprX1 was tested by *in vitro* gel mobility shift experiments. Target RNA sequences corresponding to the interaction region were produced by *in vitro* transcription using T3/T7 polymerase from cloned and amplified genes (Fig. 31).

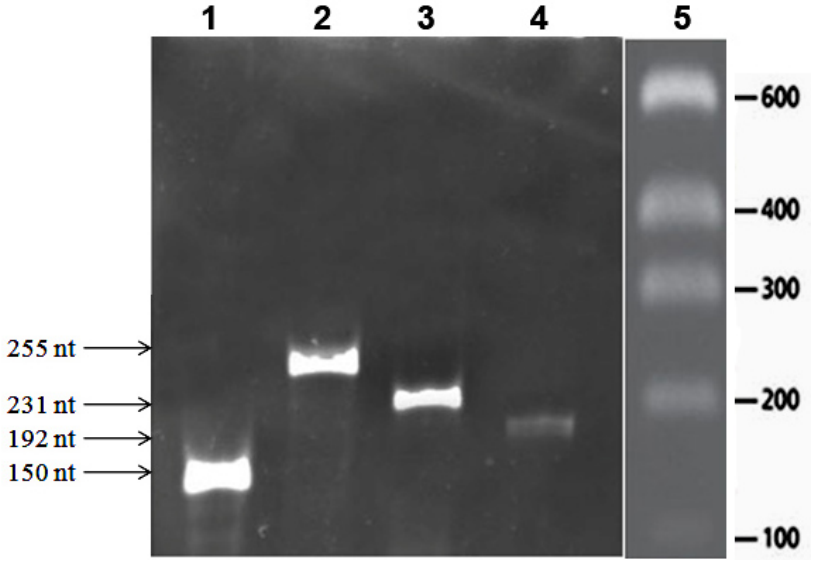

Fig. 31. *in vitro* transcription of SprX1, Hld, ClfB and PhrD RNA. Lane 1 SprX1 RNA (150 nt) and Lane 2 Hld RNA (255 nt), Lane 3 ClfB RNA (231 nt), Lane 4 PhrD RNA (192 nt) transcribed using T3 RNA polymerase and T7 RNA polymerase respectively, Lane 5 RNA marker ranging from 100-1000 bp.

Higher molecular weight complex was observed, with DIG-labelled 0.5 pmol of SprX1 and unlabelled mRNAs in the range of 0.5 to 2.5 pmol. With the 5' UTR and initial stretch of the coding sequence of the Hld mRNA interaction was best at the maximum concentration of 2.5 pmol tested (Fig. 32A), which is in agreement with the bioinformatic analysis. However, weak interaction with ClfB was observed at the molar ratio of 1:3 pmol (Fig. 32B). The addition of excess of unlabelled nonspecific competitor PhrD RNA of *Pseudomonas* origin, did not affect the duplex formation of either SprX1/Hld or SprX1/ClfB mRNA pairs in mobility shift assays.

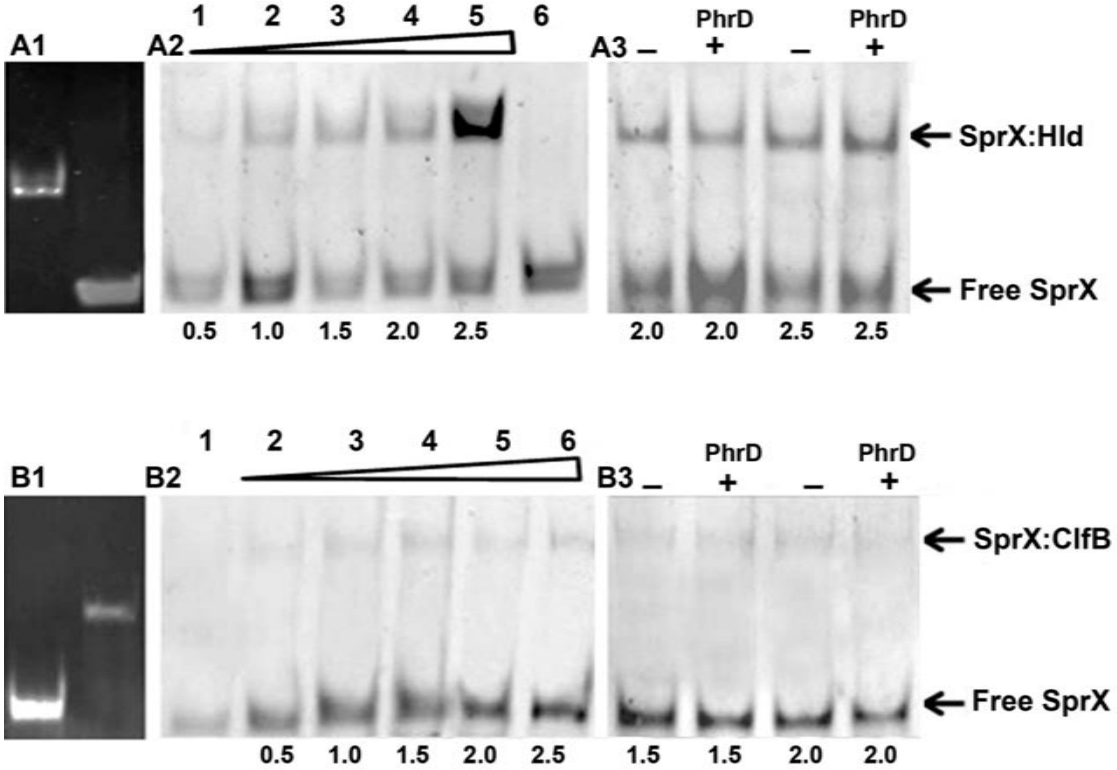

Fig. 32. Gel mobility shift assay of SprX1 with Hld/ ClfB mRNA. *in vitro* transcribed DIG-labelled SprX1 (0.5 pmol) incubated with unlabelled Hld/ ClfB RNA at 37°C for 30 min.

A1. unlabeled SprX1 and Hld run on 6% native PAGE gel,
A2. Lanes 1-5: Complex formation of SprX1 with increasing concentrations of Hld mRNA: 0.5, 1.0, 1.5, 2.0, 2.5 pmol respectively, Lane 6: SprX1 alone,
A3. Hld (2.0, 2.5 pmol) and SprX1 (0.5 pmol) interaction under 10- fold excess of nonspecific unlabeled competitor PhrD RNA with no reduction in complex formation.
B1. unlabeled SprX and ClfB run on 6% native PAGE gel,
B2. Lane 1: SprX1 alone, Lanes 2-6: Complex formation of SprX1 with increasing Concentrations of ClfB mRNA: 0.5, 1.0, 1.5, 2.0, 2.5 pmol respectively.
B3. ClfB (1.5, 2.0 pmol) and SprX1 (0.5 pmol) interaction under 10- fold excess of nonspecific unlabeled competitor PhrD RNA with no reduction in complex formation. -/+ indicates the presence and absence of PhrD.

4.2.4. Animal infection studies using Swiss albino BALB/c mice as model organism

In animal infection studies, SprX1 enhanced the virulence of *S. aureus* in mice model of infection. When mice were challenged with strains expressing altered SprX1 levels, the overexpression strain was found to be more pathogenic in comparison with the strains bearing control pCN40, knockdown or the disruption. Animals infected with overexpression strain exhibited multiple abscesses and discoloration in the kidneys, lungs, heart, liver and spleen (Fig. 33) and also showed increased levels of BUN (Fig. 34A), creatinine kinase (Fig. 34B), SGOT (Fig. 34C), SGPT (Fig. 34D) which serve as

patho-physiological markers. Bacterial load were markedly high in the kidney of mice infected with the overexpression than any other strains (Fig. 34E). These results indicate that SprX1 is essential for the virulence of *S. aureus* Newman.

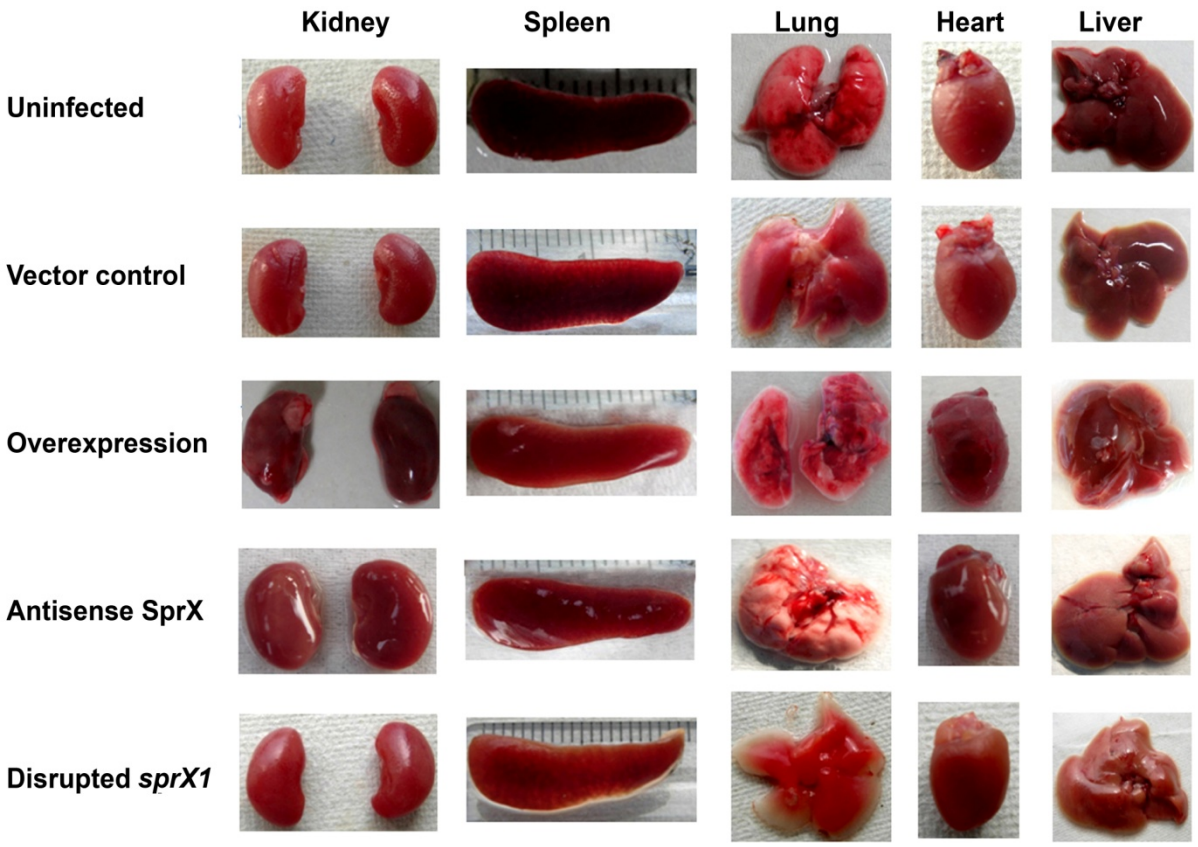

Fig. 33. Morphological changes in organs of mice infected with altered levels of SprX1in *S. aureus* Newman bearing vector control (pCN40), SprX1 overexpression (pMNSprX), antisense (pMNSprX$_{AS}$), disruption (*sprX1::kan*) and uninfected. Organs of mice infected with overexpression of SprX1 shows multiple abscess formation in kidney and discoloration of lungs, liver, heart and spleen.

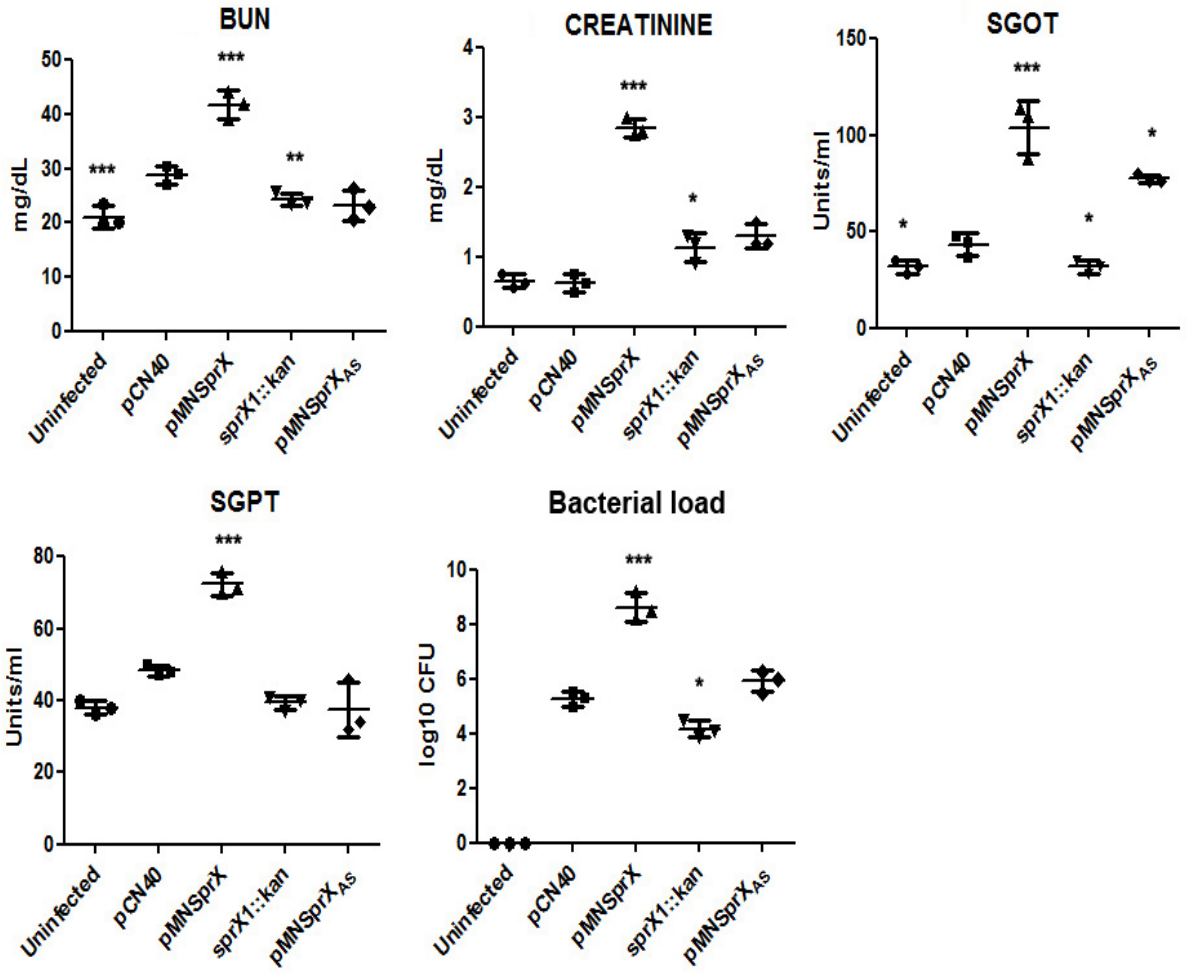

Fig. 34. Virulence studies of SprX1 in mice model of infection. Mice infected intravenously with *S. aureus* Newman strains bearing altered levels of SprX1.Biochemical parameters: A) Blood urea nitrogen (BUN), B) creatinine C) serum glutamic oxaloacetic acid transaminase (SGOT) and D) serum glutamic pyruvic acid transaminase (SGPT) of mice infected with different constructs of SprX and uninfected mice serves as negative control E) Enumeration of bacteria from kidneys of infected mice. *S. aureus* Newman strain bearing vector control (pCN40), overexpression (pMNSprX) and disruption (*sprX1::kan*) and antisense (pMNSprX$_{AS}$). Asterisks represent significant statistical differences determined for each of the parameters compared with the vector control by using two way ANOVA ***($P < 0.001$), **($P < 0.01$) and *($P < 0.05$) to interpret the data.

4.2.5. Overall influence of SprX1 on pathogenicity of *S. aureus* Newman

Small RNAs have been coupled with the regulation of gene expression by either base pairing with mRNA targets or binding to proteins, resulting in modulation of physiology of the cell and in specific, the expression profile of pathogenicity factors (Felden *et al.*, 2011). The small RNAs SprD (Chabelskaya *et al.*, 2010), SprA1/ SprA1$_{AS}$ (antisense of SprA1) (Sayed *et al.*, 2011) SprG/F (Pinel-Marie *et al.*, 2014) and SprC (Le Pabic *et al.*,

2015) which are expressed from the pathogenicity island of *S. aureus* have significant impact on virulence by modulating the expression level of target mRNAs through various networks. The sRNA SprX, which is also, encoded in the pathogenicity island of *S. aureus* Newman was characterized in this work for its functional significance. Previously, SprX has been reported to effect the expression of DNA binding protein *spoVG* that regulates bacterial resistance in the strain *S. aureus* HG001. *SpoVG*, a part of *yabJ-SpoVG* operon, is additionally involved in the regulation of the expression of extracellular nuclease, lipase, protease and capsule formation (Eyraud *et al.,* 2014). The evidence presented in this work is the first direct demonstration of its involvement in the regulation of pathogenicity factors as targets in the clinical isolate *S. aureus* Newman.

The result presented here establishes a role for SprX1 in the regulation of pathogenicity factors as targets. The identification of clumping factor B and delta hemolysin as new targets and the subsequent observation of their upregulation by SprX1 in real time PCRs and physiological assays leading to increased pathogenicity have ascertained the functional significance of this RNA. The presence of *hld* gene within the other regulatory RNA, RNAIII makes it serve as a biomarker of RNAIII (Sakoulas *et al.,* 2006), which contributes to regulation of bacterial adhesion and invasion of epithelial cells (Iyer *et al.,* 2012). Recent study indicates that RNAIII co-ordinates with the second regulatory RNA SprD in regulating the expression of single virulence factor such as immunoglobulin binding protein (*sbi*) to overcome the host defense mechanisms (Chabelskaya *et al.,* 2014). Other examples of small RNAs such as SprA1 and $SprA1_{AS}$, SprG1 and SprF1 encoded in pathogenicity island act by sRNA-sRNA interaction. $SprA1_{AS}$ acts as antisense RNA against SprA1 in regulating the cytolytic peptide translation of *S. aureus* and SprF1 prevents the expression of SprG1 encoded peptide and its RNA and protect the growth of *S. aureus* (Sayed *et al.,* 2011; Pinel-Marie *et al.,* 2014).

Clumping factor B is one of the biofilm associated genes required for the biofilm formation (Den Reijer *et al.,* 2016; Resch *et al.,* 2005; Abraham and Jefferson, 2012). The increased biofilm formation under the overexpression of SprX1 could be partly attributed to increased levels of ClfB. In addition SprX1 might mediate its effect on biofilm by increasing the stability of RNAIII which also has been reported to influence biofilm structuring and dissemination (Coelho *et al.,* 2008; Le and Otto, 2015). It would

be really interesting to study, how the effect of SprX on RNAIII would influence the expression of its several virulent targets. Whether SprX exerts its influence independently or with the help of RNAIII or *via*, global regulators is not yet understood.

The chromosomal disruption of *sprX1* was achieved by homologous recombination in *S. aureus* Newman. Out of the several mutants analysed, one mutant showed disruption in *sprX1*. The reduced expression of virulent targets as well as the decreased virulence in mice was observed in the single *sprX1* disruption mutant. Variation of SprX2 and SprX3 from SprX1 in six nucleotides resulted in poor interaction with the same targets in bioinformatic analysis, thereby signifying the role of SprX1 among the three copies in regulating the pathogenicity.

Among the other targets tested, immunoglobulin binding protein (*sbi)* and staphylocoagulase (*coa*), showed no appreciable difference in the expression, but were seen to be downregulated in the disruption of *sprX1*, indicating that SprX is not a direct regulator.

The increased pathogenicity in the mice model of infection suggested that SprX1 RNA has a great impact on virulence of clinical isolate *S. aureus* Newman. The physiological assays, expression analysis by PCRs and mice infection studies also profound the importance of SprX1. The RNA interaction studies reinforce delta hemolysin and clumping factor B as direct targets of SprX1. Taken together all these results, sRNA SprX1 in our study appears to be of great importance in maintaining the virulence of *S. aureus* Newman.

4.3. SprB- a small noncoding RNA

4.3.1. *in silico* characterization of SprB and its targets

The ncRNA SprB, approximately 110 nt long in size, is expressed from the pathogenicity island of *S. aureus* strain Newman. SprB sequence was identified and analysed in the clinical isolate Methicillin Susceptible *Staphylococcus aureus* (MSSA) strain Newman using the corresponding homologue of the reported SprB RNA in Methicillin Resistant *Staphylococcus aureus* (MRSA) strain N315 (Pichon & Felden, 2005). *sprB* gene is present within the intergenic region of a hypothetical protein and ABC transporter protein in *S. aureus* Newman (Fig. 35) and is highly conserved among the *S. aureus* strains. SprB RNA is characterized by the presence of three stem loops. The secondary structure was predicted using the software *mfold* (Fig. 36).

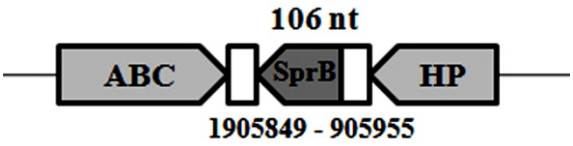

Fig. 35. Schematic representations of the genetic organization of SprB from *S. aureus* strain Newman. The ORFs, orientation of SprB gene and nucleotide (nts) numbers correspond to Newman strain.

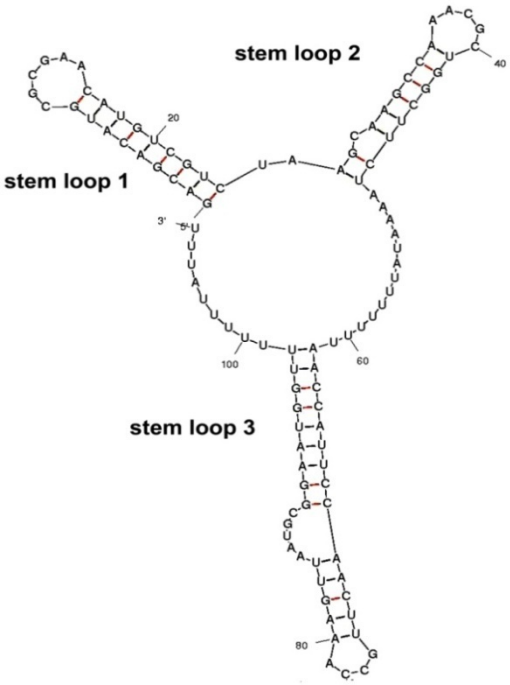

Fig. 36. Secondary structure prediction of SprB by Mfold.

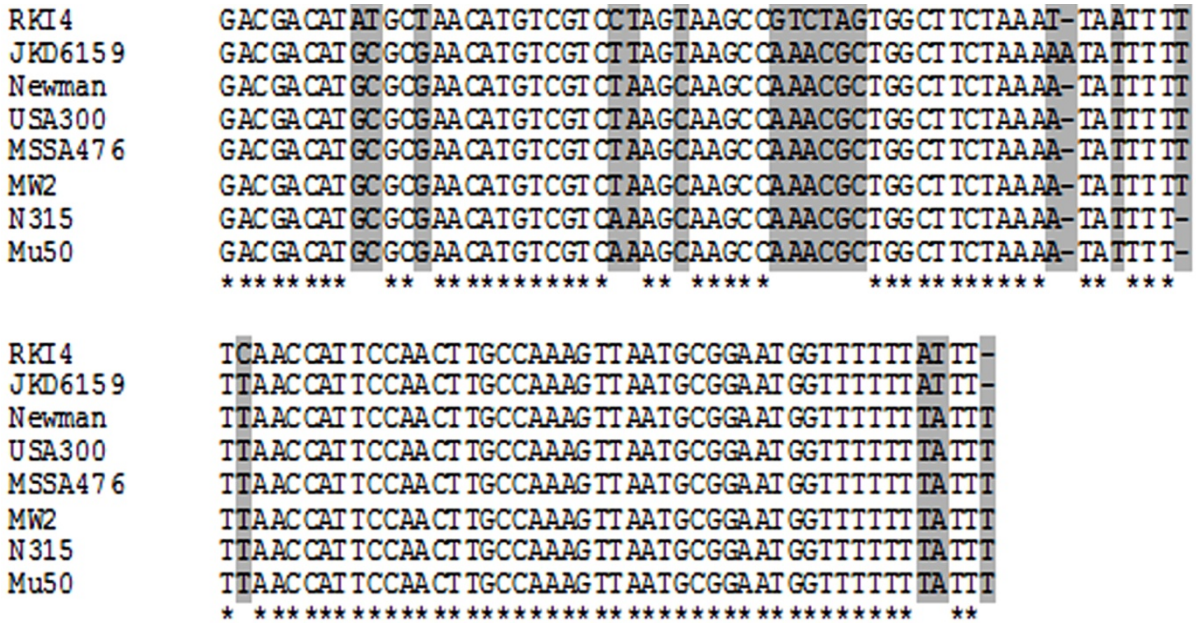

Fig. 37. Sequence alignment of SprB. Alignment of the nucleotide sequences of SprB from *S. aureus* strain Newman and other *S. aureus* strains. Identical sequences are indicated by asterisks* and non-identical sequences are highlighted in grey shade.

Among the several *S. aureus* strains analysed, two strains showed 16% variation of the sequence of SprB (Fig. 37). SprB was cloned along with its putative promoter and rho independent transcriptional terminator which were identified by using tools Softberry BPROM and Erpin respectively with default parameters (Appendix II). Bioinformatic analysis of target prediction for SprB indicates potential base pairing with multiple mRNAs such as clumping factor A, clumping factor B and staphylocoagulase which are essential for the physiological balance of the cell and were selected for the further study (Table 19).

Table 19. Base pairing interaction of SprB and its selected putative mRNA targets.

Targets of SprB	sRNA binding region	mRNA binding region	Base pairing region
coa	41-51	1585-1596	mRNA 5′ AGAAGCCAAGC 3′ |||||||| || sRNA 3′ UCUUCGGU-CG 5′
clfA	78-93	724-729	mRNA 5′ GUAUUGACUCUGGU 3′ ||||||||| |||| sRNA 3′ CGUAAUUGAAACCG 5′
clfB	48-78	-22 - +5	sRNA 5′UUCUAAAAUAUUUUUUUAACCAUUCCAACUU 3′ ||| |||||||:| ||||| ||| || mRNA 3′AAGUUUUUAUAAUGA----GGUAAAGUUAAA 5′

4.3.2. Functional characterization of SprB

4.3.2.1. Overexpression of SprB in *S. aureus* Newman

SprB was PCR amplified from wild type *S. aureus* Newman and cloned in pBluescriptKS^{+} at SmaI site. The recombinant plasmid, pBSprB (Fig. 39AB) was confirmed by DNA sequencing and further subcloned in *E. coli* - Staphylococcal shuttle vector pCN40 digested with SalI/BamHI and BamHI/KpnI to get the gene in both the sense and antisense orientation (Fig. 39CD) respectively. The obtained clones were named as pMNSprB and pMNSprB$_{AS}$ respectively (Fig. 38) were confirmed by the restriction digestion patterns and subsequently transformed in *S. aureus* Newman by passaging through intermediate host restriction deficient *S. aureus* RN4220.

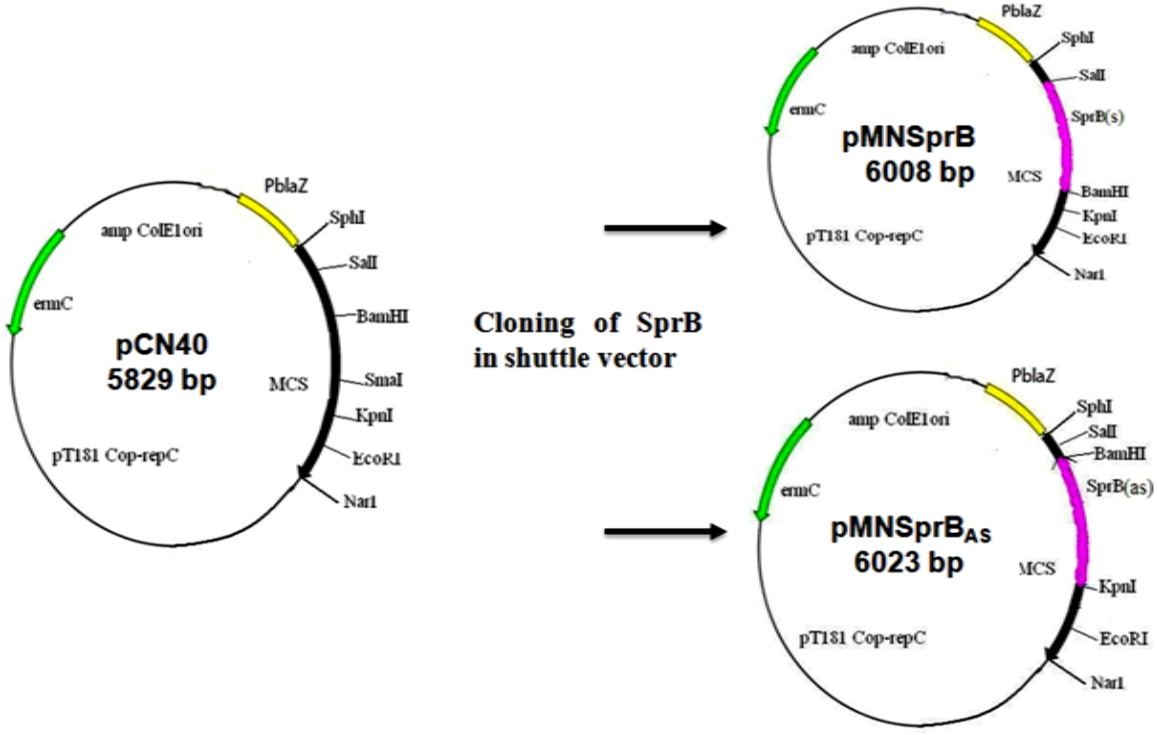

Fig. 38. Schematic representation of cloning of SprB in *E. coli* - staphylococcal vector. SprB along with its inherent promoter was subcloned in pCN40 shuttle vector using the respective enzymes SalI/BamHI and BamHI/KpnI to get the gene in both the orientation. pMNSprB, pMNSprB$_{AS}$: overexpression and antisense constructs of SprB.

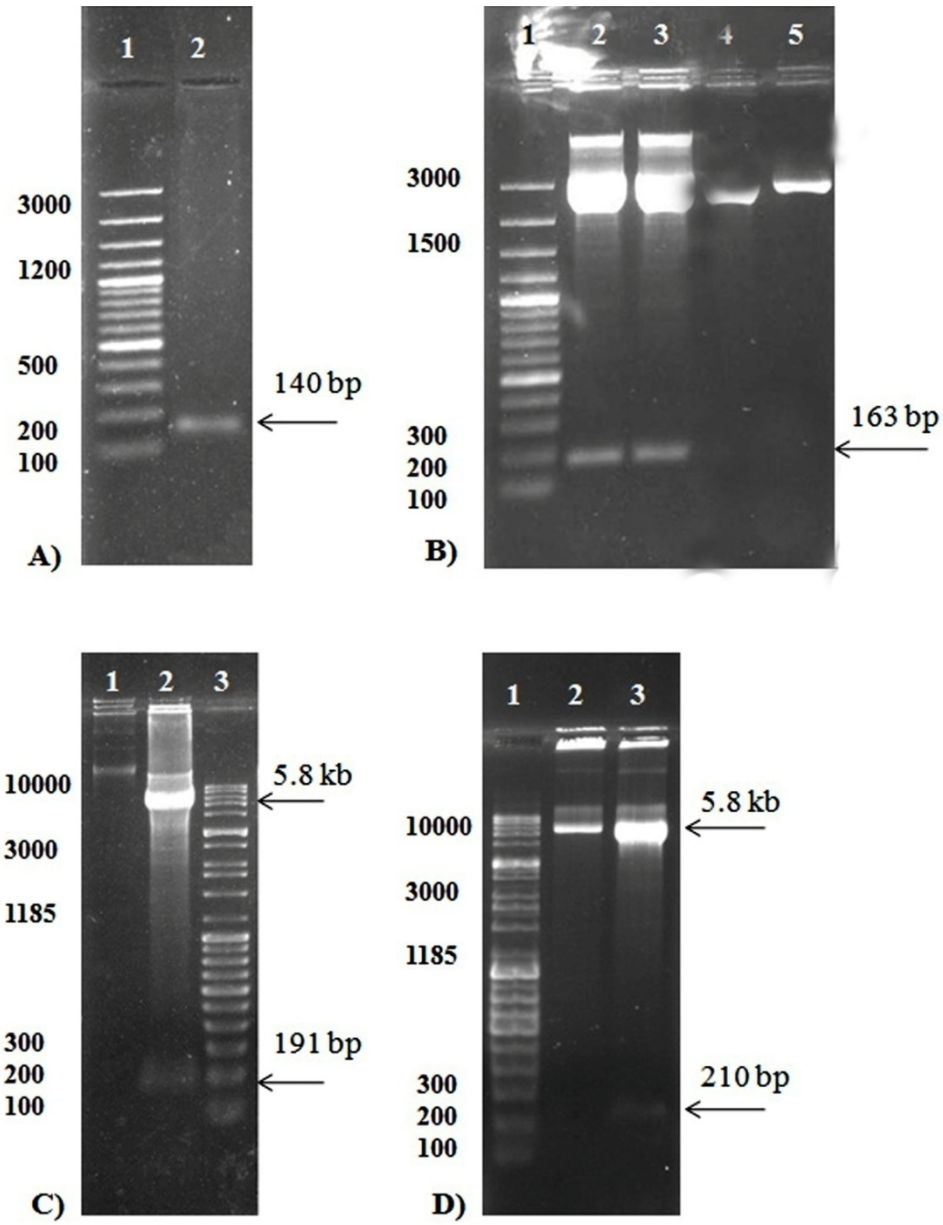

Fig. 39. PCR Amplification, cloning and subcloning of SprB.

A. and B. Lane 1: 100 bp Marker (100-3000 bp).

A. Lane 2: SprB (140 bp).

B. Lane 2,3: pBSprB showing an insert release of 163 bp, Lane 4,5: Linearization of pBSprB with BamHI, Lane 5 Linearization of pBSKS with HindIII.

C. Lane 1: undigested pMNSprB, Lane 2: pMNSprB digested with SalI/BamHI showing insert release of 191 bp, Lane 3: High range Marker (100-10000 bp).

D. Lane 1: High range Marker (100-10000 bp), Lane 2: undigested $pMNSprB_{AS}$, Lane 3: $pMNSprB_{AS}$ digested with BamHI/KpnI showing an insert release of 210 bp.

4.3.2.2. Expression analysis of SprB

The cloned SprB and its antisense strand in the multicopy vector pCN40 were expressed from its inherent native promoter or/and vector borne *blaZ* promoter respectively. Transcripts of 119 nt were obtained in Northern blot wherein an increased expression was seen at the log phase, than in the stationary phase (Fig. 40).

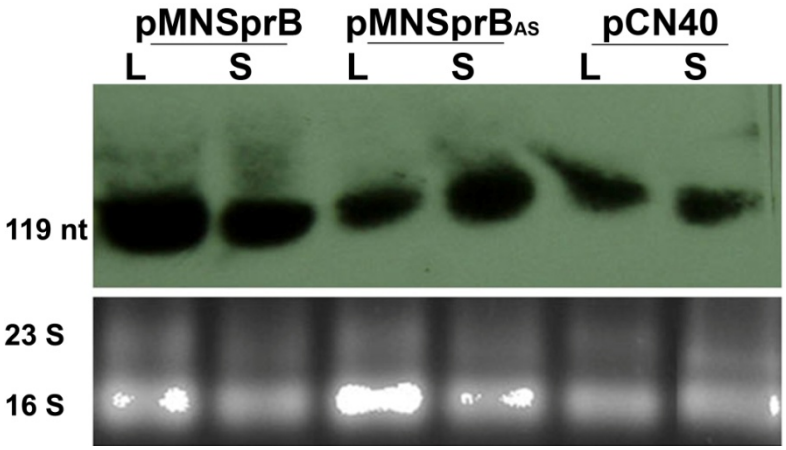

Fig. 40. Analysis of SprB overexpression by Northern blot. Total RNA isolated from the different constructs of SprB at L- log (OD_{600} 3.0) and S- stationary (OD_{600} 5.0) phase was hybridized with DIG-labelled ds SprB DNA probe. pCN40, pMNSprB, $pMNSprB_{AS}$: control vector, overexpression and antisense expression of SprB respectively. Loading control includes 23S and 16S rRNA.

4.3.2.3. Effects of SprB on various growth physiology

Strain overexpressing SprB showed delayed growth as compared to *S. aureus* strain bearing antisense SprB and the vector control (Fig. 41).

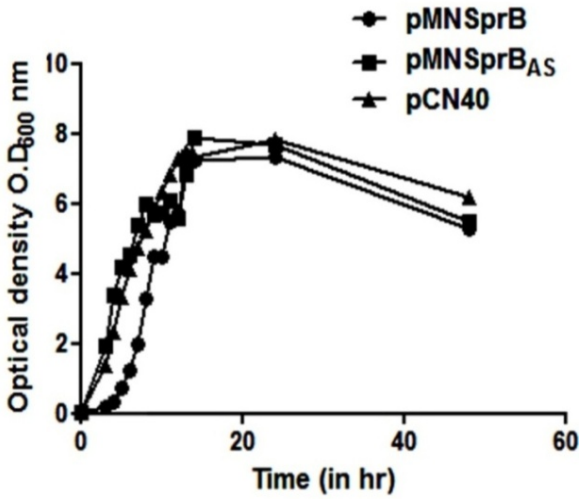

Fig. 41. Growth physiology of altered strains of *S. aureus* Newman expressing SprB. *S. aureus* Newman bearing vector pCN40, pMNSprB (overexpression) and $pMNSprX_{AS}$ (Antisense).

4.3.2.3.1. Influence of SprB on clumping factor A/B and biofilm formation

Biofilm is regulated by several factors (Resch *et al.,* 2005; Den Reijer *et al.,* 2016). These include clumping factor A/B, which were predicted as targets of SprB. Both the ClfA and ClfB mRNAs indicated potential base pairing with a stretch of 13 and 22 nt base pairing with SprB respectively (Table 19). Bioinformatic analysis suggests that the binding of SprB occurs at the 5' UTR region of ClfB which includes -22 to +5 region and in the 724 to 729 region of ClfA. The downregulation of clumping factor A and clumping factor B transcripts was observed under the overexpression of SprB in *S. aureus* Newman as measured by real time PCRs (Fig. 42).

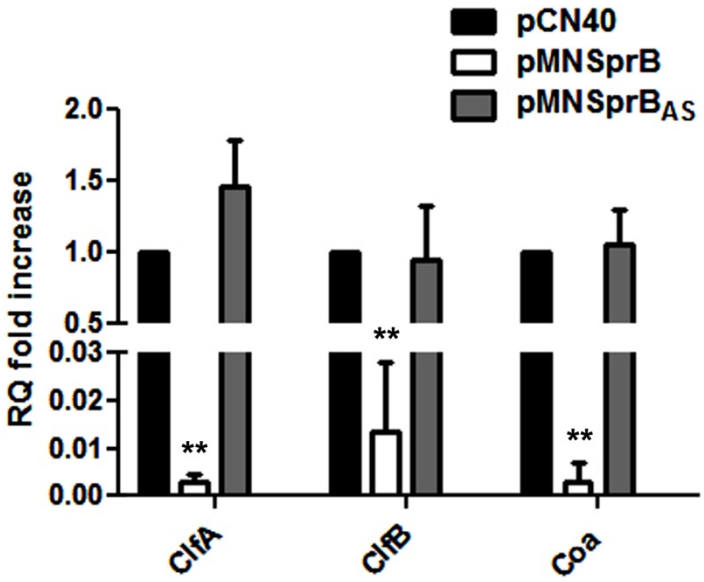

Fig. 42. Quantitative Real time PCR expression of predicted mRNA targets under the regulation of SprB. Expression profiles of target genes clumping factor A (*clfA*), clumping factor B (*clfB*), staphylocoagulase (*coa*) for the constructs *S. aureus* Newman vector pCN40 (control vector), pMNSprB (overexpression) and pMNSprB$_{AS}$ (antisense). Asterisks represent significant statistical differences determined for each of the genes compared with the vector control by using two way ANOVA **($P < 0.01$).

Biofilm formation was visualized on glass cover slip as described in 3.7.2. Strain overexpressing SprB exhibited significant reduction in biofilm formation in comparison to vector control and knock down construct which showed increased biofilms as evidenced by confocal microscopy (Fig. 43). These results were further confirmed with quantitative measurement of biofilm formation by microtiter plate assay.

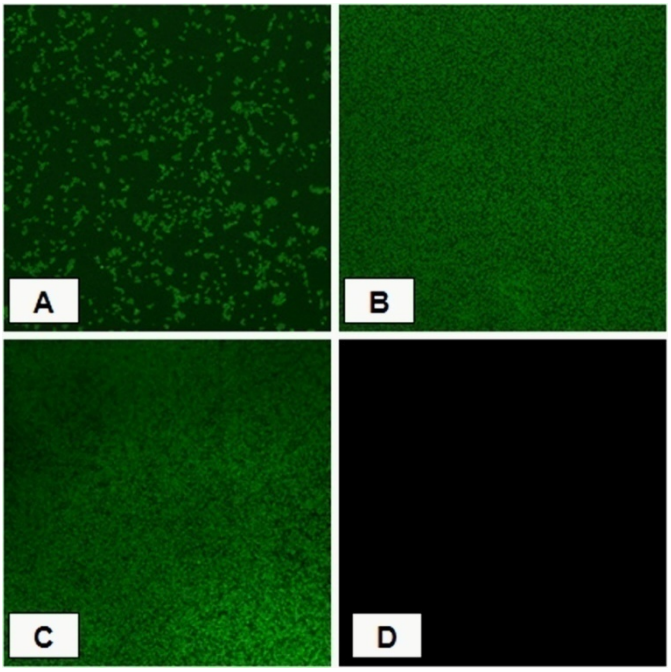

Fig. 43. Confocal laser scanning microscope (CLSM) images of biofilm formation on the glass cover slip A) under the overexpression (pMNSprB) B) antisense ($pMNSprB_{AS}$) C) Vector (pCN40) control of *S.aureus* Newman and D) shows the negative control with no cells. Cells were labelled with Fluorescein isothiocyanate (FITC).

Modified *S. aureus* cells overexpressing SprB displayed reduced adherence on the microtiter plate, as measured quantitatively by staining the adhered cells with crystal violet at 570 nm (Fig. 44). The poorer biofilm formation even in the presence of the inducer glucose, suggests the potent role of SprB in the staphylococcal infection. The clumping factors ClfA and ClfB which are the surface associated fibrinogen binding proteins of *S. aureus*, attached to the cell wall and mediate adherence of bacteria to immobilized fibrinogen, blood clots, conditioned biomaterial *ex vivo*, and to thrombi on damaged heart valves.

These proteins also promote clumping of bacteria in the presence of soluble fibrinogen (McAleese *et al.*, 2001). Clumping factor plays a specific role in the pathogenesis of endocarditis in *Staphylococcus aureus* Newman (Moreillon *et al.*, 1995). Thus the reduced expression of both clumping factor B and clumping factor A under the overexpression of SprB, illustrates the significance of SprB on biofilm formation and hence may reduce staphylococcal colony formation and invasiveness in the host.

.

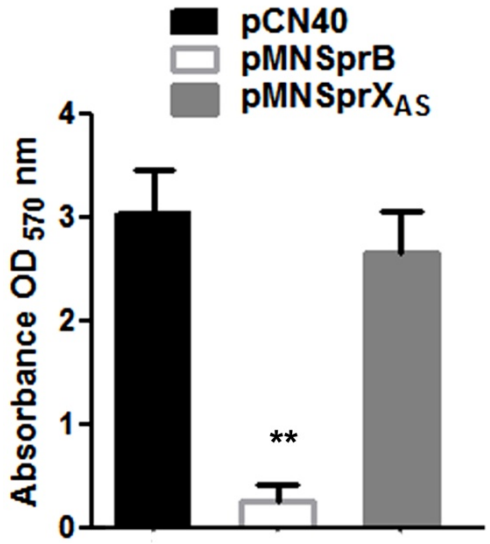

Fig. 44. Quantitative measurement of biofilm by microtiter plate assay. Microtiter plate assay of biofilm formation of different constructs of SprB in *S. aureus* Newman: overexpression (pMNSprB), antisense (pMNSprB$_{AS}$) and vector (pCN40) control. Error bars depicts four biological replicates. Statistical difference **($P < 0.05$) between the constructs was determined by using one way ANOVA on comparison with the vector control.

4.3.2.3.2. Influence of SprB on staphylocoagulase

Staphylocoagulase promotes clotting of plasma or blood and is required for the abscess formation and persistence in host tissues (Cheng *et al.,* 2010). The coagulase expression is both positively and negatively controlled by an *agr* dependent mechanism (Lebeau, 1994). Quantitative measurement of staphylocoagulase (*coa*) transcript by real time PCRs showed significant downregulation under the overexpression of SprB in *S. aureus* Newman (Fig. 42), thus indicating the importance of SprB on the regulation of staphylocoagulase. However, there is no significant increase in the *coa* levels in the constructs bearing antisense of SprB compared with the vector control.

4.3.2.3. Influence of SprB on staphyloxanthin pigment production

The orange and yellow pigments called as staphyloxanthin that are produced by golden colonies of *Staphylococcus aureus* are the products of a C30 triterpenoid biosynthetic pathway (Kim & Lee, 2012). Although mRNAs corresponding to staphyloxanthin biosynthetic enzymes were not among the predicted targets in bioinformatic analysis for SprB, production of carotenoid pigment was reduced to 32.4% over the period of 14 days (Fig. 45) in the strain overexpressing SprB in comparison to the vector control.

Further, although there is an overall reduction of pigment production in the control and test, nevertheless the level in the test is still remains lower than in the control. This decrease in staphyloxanthin pigment production was marked during incubation at cold temperature 4°C. The staphyloxanthin pigment production in *S. aureus* is mediated by the co-ordinated involvement of several factors including sigma factor B (*sigB)* dependent stress response genes, cold shock protein A (*cspA*) and also a change in the metabolic pathways such as TCA cycle, purine biosynthesis and oxidative phosphorylation enhances the pigmentation (Lan *et al.*, 2010). Further studies are required to determine which genes are being directly influenced by SprB to bring about the above observations.

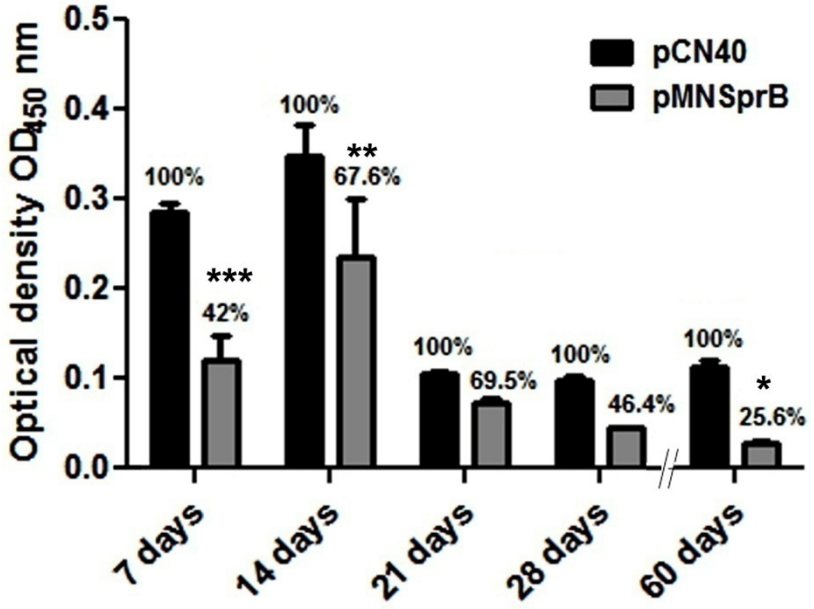

Fig. 45. Influence of SprB on staphyloxanthin pigment production. Pigment production by different constructs of SprB in *S.aureus* Newman bearing pCN40 (control), pMNSprB (overexpression). Asterisks represent significant statistical differences determined for each time intervals compared with the vector control by using two way ANOVA ***(P<0.001), **(P<0.01) and *(P<0.05).

4.3.2.3.4. Influence of SprB on antibiotic susceptibility

Susceptibility to antibiotics by *S. aureus* expressing modified levels of SprB was studied by Kirby-Bauer disc diffusion method. It was observed that *S. aureus* strain bearing SprB overexpression construct showed marked increase in resistance to four *β*-lactam antibiotics namely amyoxicillin, penicillin, penicillin V and ampicillin that inhibit the biosynthesis of bacterial cell wall, conversely increased sensitivity to aminoglycoside

antibiotic gentamycin and *β*-lactam antibiotic cloxacillin was seen, when compared with the vector control (Fig. 46). Several ncRNAs are reported to involve in influencing bacterial resistance to antibiotics by interfering with the activities of antibiotics such as blocking of transcriptional machinery and protein synthesis of bacteria (Eyraud *et al.*, 2014; Lalaouna *et al.*, 2014). It affects antibacterial resistance by regulating the production of protein pumps that forcibly remove the antibiotic from the cell. The active pumping of antibiotics out of the cell is carried out by efflux pump systems (Li and Nikaido, 2009). Bioinformatic analysis shows *mmpL* gene encoding quinolones and *β*-lactams drug efflux pumps as one of the putative targets of SprB. The regulation of antibiotic resistance in *S. aureus* may be attributed to this gene. Recent studies in *S. aureus* strain HG001 has shown SprX to be involved in glycopeptide and oxacillin resistance by inhibiting SpoVG protein synthesis, a protein encoded by the *yabJ-spoVG* operon responsible for its resistance (Eyraud *et al.*, 2014).

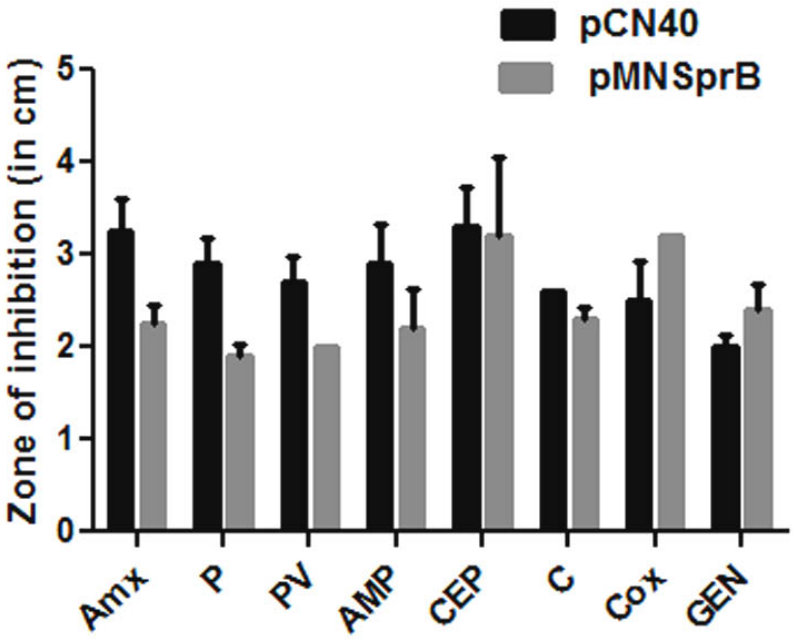

Fig. 46. Influence of altered levels of SprB on antibiotic susceptibility. *S. aureus* Newman bearing pCN40 (control) and pMNSprB (overexpression) constructs were tested for antibiotic susceptibility using discs of fixed concentration: Amyoxicillin (Amx)- 10 µg, Penicillin (P)- 2 µg, Penicillin V (PV)- 3 µg, Ampicillin (AMP)- 10 µg, Cephalothrin (CEP)- 30 µg, Chloramphenicol (C)- 30 µg, Cloxacillin (Cox)- 5 µg, Gentamycin (GEN)- 10 µg. Statistical differences was determined using two way ANOVA.

The other examples include NrrF sRNA in *N. gonorrhoeae* reduces *mtrF* mRNA levels which are responsible for coding inner membrane protein MtrF and MtrCDE efflux

pump that results in resisting various hydrophobic antimicrobials, including penicillin and erythromycin (Jackson *et al.,* 2013). The overexpression of sRNA DsrA is found to induce multidrug resistance in *E. coli.* DsrA triggers the expression of genes encoding the MdtEF multidrug efflux pump and thus affects antibiotic susceptibility (Nishino *et al.*, 2011). More interestingly, it was found that blocking the production of sRNA leaves the cell more vulnerable to antibiotic attack (Lalaouna *et al.*, 2014). Thus it suggests that SprB may play significant role in mediating antibiotic resistance by regulating important cellular factors.

4.3.3. Virulence studies of SprB in mice model of infection

In animal infection studies, mice was challenged with *S. aureus* strains bearing overexpression of SprB, pCN40 (vector control) and knockdown constructs. The infectivity was indicated with the observations on morphological features of organs, pathophysiological parameters and bacterial enumeration as in section 3.10.

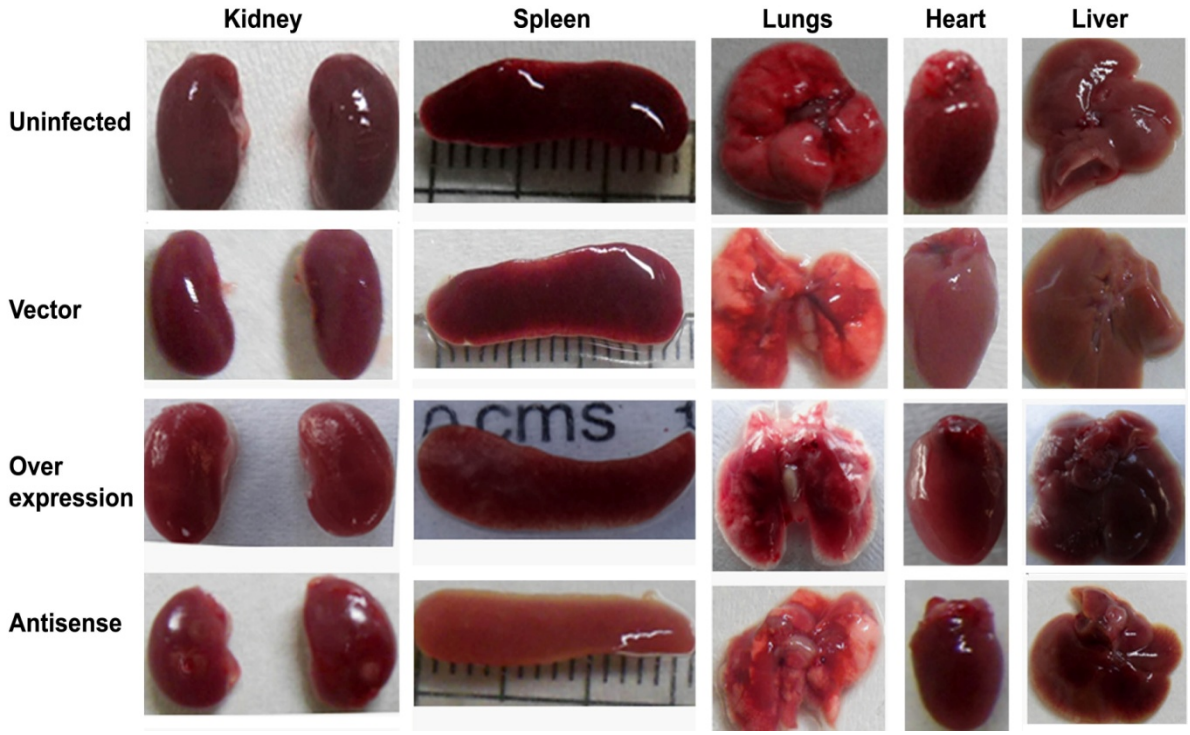

Fig. 47. Morphological changes in organs of mice infected with altered levels of SprB in *S. aureus* Newman bearing vector control (pCN40), SprB overexpression (pMNSprB), antisense ($pMNSprB_{AS}$) and uninfected mice serves as control. Organs of mice infected with antisense of SprB shows multiple abscess formation in kidneys and discoloration of lungs and spleen.

Mice infected with SprB overexpression strain showed no significant differences in organ biomarkers and bacterial load with respect to the vector control, indicating that SprB did not have much influence on pathogenicity. However, when mice infected with the knockdown strain exhibited marked abscesses formation in kidneys, discoloration of spleen and lungs (Fig. 47), increased levels of creatinine, SGOT, SGPT (Fig. 48) and high bacterial load than any other strains.

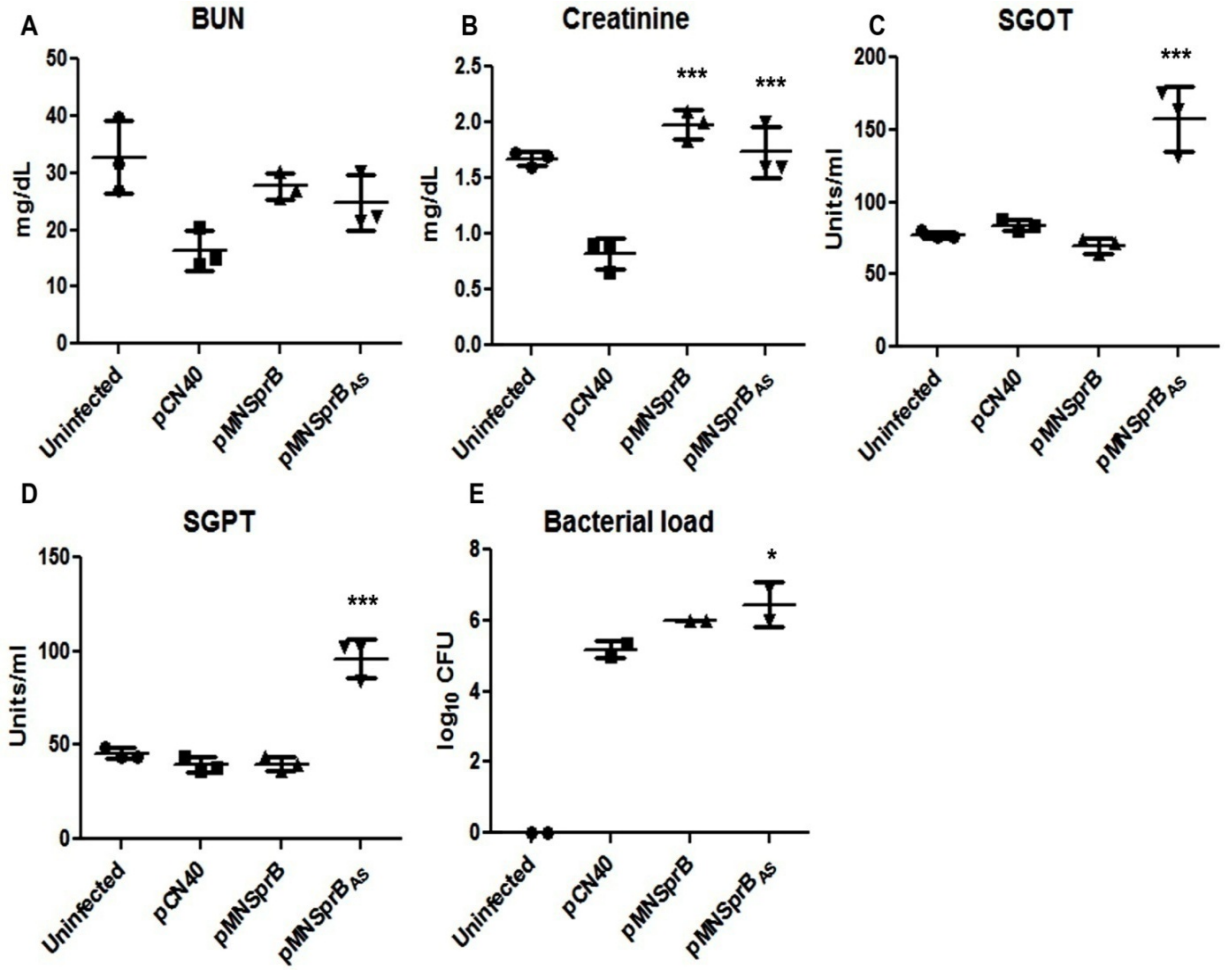

Fig. 48. Virulence studies of SprB in mice model of infection. Mice were infected intravenously with *S. aureus* Newman strains bearing altered levels of SprB. A) Blood urea nitrogen (BUN) B) creatinine C) serum glutamic-oxaloacetic acid transaminase (SGOT) D) serum glutamic-pyruvic acid transaminase (SGPT) and E) Bacterial enumeration from kidneys of infected mice. pMNSprB, pMNSprB$_{AS}$ and pCN40: SprB overexpression, antisense and vector control respectively. Asterisks* represent significant statistical differences ($P < 0.05$) determined for each of the parameters compared with the vector control by using one way ANOVA to interpret the data.

4.3.4. Overall influence of SprB in *S. aureus* Newman

Small noncoding RNA SprB, which is encoded in the pathogenicity island, was characterized for its functional significance in pathogenicity. Several studies have shown how sRNAs expressed from Pathogenicity Island in mobile elements, which encode for virulence factors and resistance gene, affected the translational regulation of genes of the core genome (Fechter *et al.,* 2014).

Among the two regulatory ncRNAs studied here, SprB has converse effect in comparison to SprX1, which elevated the expression of clumping factor A/B and increased the biofilm formation. It is interesting to study how two RNAs works in an opposite manner in regulating staphylococcal colonization.

It is reported that strains producing more carotenoid pigments show more pathogenicity (Mishra *et al.,* 2011). *S. aureus* utilizes its golden carotenoid pigment to resist oxidation based clearance mechanisms of the host innate immune system (Mishra *et al.,* 2011). The decreased pigment production in strain overexpressing SprB suggests that it may have less pathogenicity in the host as observed in this study. A previous study also indicates that *S. aureus* mutants with disrupted carotenoid biosynthesis are more susceptible to oxidant killing, has impaired neutrophil survival and is less pathogenic in a mouse subcutaneous abscess model (Katzif *et al.,* 2005).

The increased resistance to beta-lactam antibiotics such as penicillin, penicillin V, amoxicillin, ampicillin and increased sensitivity to gentamycin and cloxacillin was noted in the strains overexpressing SprB. Unravelling the functions of sRNAs in antibiotic resistance and virulence will provide fundamental knowledge that can be used to develop next-generation antibacterial agent using sRNAs as targets in future (Lalaouna *et al.,* 2014).

Although antisense transcript was detected in Northern blot, there was no reverse effect on the target genes and biofilms, as compared to the overexpression of SprB construct. It can be speculated that due to different secondary structure of antisense SprB, it may be less efficient in base pairing and knocking down SprB expression. This in turn may have an effect on different targets which are not predictable.

With the reduced pigment production and biofilm formation of strain overexpressing SprB in the physiological assays, it was anticipated that, this strain would be less pathogenic. However, in the mice infection studies, SprB did not have much influence on pathogenicity, although, mice infected with strain expressing antisense SprB showed organ disintegration and significant differences on biochemical parameters. This could be attributed to involvement of other regulatory factors for successful infection.